OFFICE OF CIVILIAN RADIOACTIVE WASTE MANAGEMENT
ANALYSIS/MODEL COVER SHEET
Complete Only Applicable Items

1. QA: QA
Page: 1 of: 38

2. ☒ Analysis — Check all that apply

Type of Analysis	☐ Engineering ☒ Performance Assessment ☐ Scientific
Intended Use of Analysis	☐ Input to Calculation ☒ Input to another Analysis or Model ☐ Input to Technical Document
Describe use:	
Input to TSPA for Site Recommendation	

3. ☒ Model — Check all that apply

Type of Model	☐ Conceptual Model ☒ Abstraction Model ☐ Mathematical Model ☐ System Model ☐ Process Model
Intended Use of Model	☐ Input to Calculation ☒ Input to another Model or Analysis ☐ Input to Technical Document
Describe use:	
Input to TSPA for Site Recommendation	

4. Title:

Abstraction of Drift Seepage

5. Document Identifier (including Rev. No. and Change No., if applicable):

ANL-NBS-MD-000005 REV 00

6. Total Attachments:	7. Attachment Numbers - No. of Pages in Each:
3	I – 14 pp., II – 8 pp., III – 1 p.

	Printed Name	Signature	Date
8. Originator	Michael L. Wilson	Michael Wilson	3/09/00
9. Checker	Mark Bandurraga	Peter Persoff for Mark Bandurraga	3/9/00
10. Lead/Supervisor	Michael L. Wilson	Michael Wilson	3/10/00
11. Responsible Manager	Clifford K. Ho	Clifford K. Ho	3/10/00

12. Remarks:

Clifford Ho provided the "weep" analysis of the UZ flow fields that is documented in Section 6.3.3 of this report

Final check by Peter Persoff.

Initial Issue.

OFFICE OF CIVILIAN RADIOACTIVE WASTE MANAGEMENT
ANALYSIS/MODEL REVISION RECORD
Complete Only Applicable Items

2. Analysis or Model Title:

Abstraction of Drift Seepage

3. Document Identifier (including Rev. No. and Change No., if applicable):

ANL-NBS-MD-000005 REV 00

4. Revision/Change No.	5. Description of Revision/Change
00	Initial issue

CONTENTS

Page

FIGURES

Page

TABLES

Page

1. PURPOSE

Drift seepage refers to flow of liquid water into repository emplacement drifts, where it can potentially contribute to degradation of the engineered systems and release and transport of radionuclides within the drifts. Because of these important effects, seepage into drifts is listed as a "principal factor for the post-closure safety case" in the screening criteria for grading of data in Attachment 6 of AP-3.15Q, Rev. 1/ICN 1, *Managing Technical Product Inputs*. Abstraction refers to distillation of the essential components of a process model into a form suitable for use in a total-system performance assessment (TSPA). Thus, the purpose of this analysis/model is to put the information generated by the seepage process modeling in a form appropriate for use in the TSPA for the Site Recommendation. This report also supports the Unsaturated-Zone Flow and Transport Process Model Report. The approach of the analysis is to generate probability distributions that represent the uncertainty and spatial variability of seepage. Seepage can then be treated as a stochastic quantity in TSPA simulations by sampling values from the probability distributions. In defining the probability distributions, the dependence of seepage on key input parameters (including percolation flux, fracture permeability, and fracture air-entry parameter) is taken into account, and the influence of perturbing physical processes (including drift degradation, thermal processes, and flow focusing) is considered.

Constraints and limitations of this work include the unqualified status of the input data used in the analysis/model (see Section 4.1). Once these source data are qualified, the results of this analysis/model can be considered qualified. Until then, the information developed from this analysis/model must be considered unqualified. The perturbing physical processes mentioned above are only included in the analysis/model in an approximate manner. However, the approximations are chosen so as to overestimate the amount of seepage, so that the final abstraction should produce conservative results in the TSPA. Another limitation is that the seepage data available at present all come from a geohydrologic unit, the Topopah Spring middle nonlithophysal unit, which comprises only a small portion of the planned repository. If data were available to represent the rest of the repository area, it might be possible to reduce the uncertainty in the results.

Planning of this analysis/model can be found in the following Work Direction and Planning Document: *Seepage Models for PA and Abstraction of Drift Seepage & Drift-Scale Coupled Processes (Rev. 02), ID: U4000, U6020; Activity: SPP5210, SPP5290* (CRWMS M&O 1999a). Note that this planning document contains tasks identified for both Performance Assessment Operations (PAO) and Natural Environment Program Operations (NEPO). Only the PAO tasks are documented here. A separate development plan was later issued for the NEPO work (CRWMS M&O 1999b) and that work is documented in a separate report (CRWMS M&O 2000a). The work plan calls for determining an appropriate abstraction methodology, determining uncertainties in seepage, and providing probability distributions of seepage. These are all discussed in detail in this report. In addition, the work plan calls for evaluation of effects of episodic flow and thermal-hydrologic-chemical alteration of hydrologic properties. As discussed in Section 5, these effects are not addressed in detail in this report because they can be argued to be insignificant. Effects of thermal-mechanical alteration of hydrologic properties are also not addressed in detail in this report because suitable process-model results are not available at this time.

2. QUALITY ASSURANCE

This analysis/model was prepared in accordance with the Civilian Radioactive Waste Management System (CRWMS) Quality Assurance program. The PAO responsible manager has evaluated this activity in accordance with QAP-2-0, *Conduct of Activities*. The QAP-2-0 activity evaluation (CRWMS M&O 1999c) determined that the development of this analysis/model is subject to the requirements in the *Quality Assurance Requirements and Description* (DOE 2000). The analysis was conducted and this report developed in accordance with AP-3.10Q, *Analyses and Models*.

3. COMPUTER SOFTWARE AND MODEL USAGE

A software routine was used to calculate the spacing between actively flowing fractures in the site-scale unsaturated-zone (UZ) flow model (Section 6.3.3). This routine was checked as part of this analysis/model to ensure that it provides correct results for the input files used. The use and documentation of this software routine complies with Section 5.1.1 of AP-SI.1Q Rev. 2/ICN 4, *Software Management*.

Table 1. Software Routine Used in this Analysis/Model

Software Routine	Computer Platform/ Operating System	Comments
T2WEEP v. 1.0	Sun UltraSPARC SunOS 5.7	This software routine extracts percolation fluxes and weep spacings from TOUGH2 flow fields. It was compiled using FORTRAN 77 on the Sun OS 5.7 server (worf) at Sandia National Laboratories. As part of this analysis/model, the results from the software routine T2WEEP v. 1.0 were visually inspected to ensure that the routine provided correct results for the input files and formulation that were used (see Section 6.3.3.1 and Attachment I). The listing of this routine is in Attachment I. All files associated with this software routine have been submitted to the Technical Data Management System under DTN: SN9912T0511599.002.

Aside from the above software routine, only off-the-shelf commercially available software was used for this analysis/model. Calculations and plots were made using Microsoft Excel 97 SR-2 (i). The results were spot-checked by hand to ensure that the results were correct. The computer used was a Dell Precision 410 with Pentium II processor, running Microsoft Windows NT 4.00.1381.

4. INPUTS

4.1 DATA AND PARAMETERS

Table 2 summarizes the input data used in this analysis/model. Some of the data were originally obtained via Input Transmittal (per AP-3.14Q, *Transmittal of Input*), but they are now in the Technical Data Management System (TDMS) and it has been confirmed that the TDMS data are the same as the data obtained by input transmittal. The drift and waste-package geometry and

repository outline (items 2, 13), seepage results (item 1), flow fields (items 8–10), and mesh (item 11) are not qualified. The rest of the data are qualified, but are either in the process of being reverified or dependent on other data that are being reverified. Details of the input status and TBV numbers are given in the Document Input Reference System (DIRS) for this report.

Table 2. Input Data Used in this Analysis/Model

Item	Description	Data Tracking Number (DTN)	Comments
1	Seepage Results	LB991101233129.002	Seepage percentage for suite of cases
2	Drift and Waste-Package Geometry	SN9908T0872799.004	Drift diameter, average waste-package length, waste-package spacing
3	Air-Permeability Data	LB990901233124.004	Post-construction permeability
4	Seepage Calibration Results	LB990831012027.001	Calibrated fracture alpha parameter
5	Site-Scale Calibrated Properties	LB997141233129.001	Base-infiltration case: gamma parameter, residual liquid fracture saturation
6		LB997141233129.002	High-infiltration case: gamma parameter, residual liquid fracture saturation
7		LB997141233129.003	Low-infiltration case: gamma parameter, residual liquid fracture saturation
8	Flow Field Simulations for Infiltration Scenarios	LB990801233129.007	Glacial-transition low-infiltration flow field
9		LB990801233129.009	Glacial-transition base-infiltration flow field
10		LB990801233129.011	Glacial-transition high-infiltration flow field
11	Mesh	LB990701233129.001	Mesh file used with flow fields (3d2kpa_pc1.mesh)
12	Hydrologic Properties	LB990501233129.001	Uncalibrated constant properties for all units: fracture frequency, fracture/matrix area
13	Repository Outline	SN9907T0872799.001	Coordinates for repository outline

4.2 CRITERIA

Although no specific criteria have been identified in project requirements documents (e.g., System Description Documents) as applicable to this activity, the seepage-abstraction analysis/model supports the definition of hydrologic parameters for performance assessment as required by the interim guidance from the Department of Energy pending issuance of new regulations by the Nuclear Regulatory Commission (Dyer 1999). Relevant requirements for performance assessment from Section 114 of that document are: "Any performance assessment

used to demonstrate compliance with Sec. 113(b) shall: (a) Include data related to the geology, hydrology, and geochemistry ... used to define parameters and conceptual models used in the assessment. (b) Account for uncertainties and variabilities in parameter values and provide the technical basis for parameter ranges, probability distributions, or bounding values used in the performance assessment. ... (g) Provide the technical basis for models used in the performance assessment such as comparisons made with outputs of detailed process-level models ... ."

4.3 CODES AND STANDARDS

No specific, formally established standards have been identified as applying to this analysis/model activity.

5. ASSUMPTIONS

The abstraction of seepage into drifts that is documented in this report is based directly on results of the Seepage Model for PA (CRWMS M&O 2000a). Assumptions regarding the development of that model and its results are documented in Section 5 of that report.

Assumptions that pertain to this abstraction analysis/model are as follows.

1. *Seepage can be treated as a random process.* The locations and amount of seepage into drifts are sensitive to the heterogeneity in fracture properties around the drifts (CRWMS M&O 2000a, Sections 6.6.5 and 6.7). The heterogeneity is not knowable in detail, but rather is typically described using geostatistics (CRWMS M&O 2000a, Section 6.3). Thus, it is appropriate to treat seepage probabilistically in TSPA simulations. This is a basic assumption that applies throughout the report.

2. *The extent of flow focusing can be estimated using the active-fracture model.* The "active fracture" conceptual flow model (Liu et al. 1998) that is being used for site-scale UZ flow calculations is based on the concept that flow is channeled in fractures, so that only some fractures are actively flowing. There are no data on the spacing of active flow channels or the extent of flow focusing, but the conceptual model can provide an estimate of the degree of channeling in fractures and thus the degree of intermediate-scale focusing of flow. Spacing between active flow channels is calculated assuming discrete flow in vertical fractures that are either saturated or unsaturated, yielding two bounding conditions for "weep" spacings. Explanation and justification for the active-fracture model are given in the paper (Liu et al. 1998); use of the active-fracture model to estimate focusing of flow above drifts is discussed in Section 6.3.3 of this report.

3. *Effects of episodic flow on seepage can be neglected.* While seepage under conditions of episodic flow can be evaluated (CRWMS M&O 2000a, Section 6.6.7), there are no data to indicate that significant amounts of episodic flow exist at the repository depth in Yucca Mountain. Bomb-pulse ^{36}Cl found in the exploratory studies facility (ESF) is widely regarded as indirect evidence for the existence of some episodic flow, but it is generally believed that only a small fraction of the water is involved (Bodvarsson et al. 1997, Chapter 16). No data are available to quantify the fraction of water that might be involved in episodic flow at the repository. Theoretical studies have shown that the Paintbrush nonwelded

geohydrologic unit above the repository damps out flow transients (e.g., CRWMS M&O 1998, Section 2.4.2.8). Additional documentation of the importance or unimportance of episodic flow is being developed for the screening of features, events, and processes (FEPs) for UZ flow and transport (CRWMS M&O 1999d, FEP number 2.2.07.05.00). There is some additional discussion in Section 6.3.4 of this report.

4. *Thermal-mechanical and thermal-chemical effects on seepage can be neglected*. Changes in hydrologic properties around the emplacement drifts caused by thermal-mechanical stresses and by thermal-chemical dissolution and precipitation processes are of potential concern. A fully coupled drift-scale thermal-hydrologic-chemical model has recently been developed (CRWMS M&O 2000b). Simulations with that model show only very small changes in hydrologic properties (at most 0.5% change in fracture porosity: CRWMS M&O 2000b, Section 6.3.5). These results justify neglecting thermal-chemical effects on seepage. A similar evaluation of thermal-mechanical effects on seepage is not yet available. Documentation of the importance or unimportance of thermal-hydrologic-mechanical and thermal-hydrologic-chemical processes is being developed for the screening of FEPs for UZ flow and transport (CRWMS M&O 1999d, FEP numbers 2.2.10.01.00, 2.2.10.04.00, and 2.2.10.06.00) and for thermal hydrology (CRWMS M&O 1999e, same FEP numbers). Because results are not available, thermal-mechanical effects are not included in the seepage abstraction at this time; however, this assumption requires confirmation. The assumption that thermal-mechanical effects on seepage can be neglected has been assigned TBV #3964. The assumption of neglecting thermal-mechanical effects applies throughout the report.

5. *Seepage for non-convergent simulations can be bounded by 100% of the flow above a drift segment*. As discussed in Section 6.2.1, there were convergence problems with some of the seepage process-model simulations. In those cases, it is assumed that 100% of the flow above the footprint of the drift seeps into the drift. This assumption is intended to be conservative. In principle, it could be possible for seepage percentage to be somewhat higher than 100%, but such a result is not expected, and seepage even as high as 100% of the flow above the drift was not observed in any of the simulations (CRWMS M&O 2000a, Tables 4–8; Table 2 of this report, item 1).

6. *The standard deviation of* $\log(\bar{k}/\alpha)$ *can be approximated by the standard deviation of* $\log(\bar{k})$. For a full explanation of these terms, see Section 6.2.2. There it is explained that the standard deviation of the log of the ratio of permeability to α parameter, $\sigma_{\log(k/\alpha)}$, is taken to be equal to the standard deviation of the log of permeability alone, $\sigma_{\log(k)}$. This assumption is necessary because no data are available regarding the standard deviation of the α parameter. It is also explained, at the end of Section 6.2.2, that the choice is expected to be conservative, basically because permeability and fracture α parameter are likely to be correlated, and correlations tend to decrease the standard deviation of the log of their ratio (see Table 6).

7. *Seepage is increased by 55% to account for the effects of drift degradation and rock bolts, and by another 10% to account for possible effects of correlation between* α *and k*. These assumptions are discussed in detail in Sections 6.3.1 and 6.3.2, where it is argued that these adjustments are conservative.

The only one of these assumptions that is considered to need further confirmation is part of number 4: the neglect of thermal-mechanical effects. As discussed above, the others are considered to be justified as either reasonable or conservative, such that additional confirmation with respect to this analysis/model is not necessary.

6. ANALYSIS/MODEL

6.1 OVERVIEW

The abstraction of drift seepage is based on the results of the Seepage Model for PA (CRWMS M&O 2000a). This is a drift-scale UZ flow model, which simulates flow through a fracture continuum with geostatistically-defined hydrologic properties. Possible alternative conceptual models are discussed in the model report (CRWMS M&O 2000a, Section 6.7).

The abstraction method is an extension of the method used for the TSPA for the Viability Assessment (DOE 1998, Sections 3.1.1.4, 3.1.2.4, and 3.1.3.3; CRWMS M&O 1998, Sections 2.2.4, 2.4.4, and 2.5.2). The objective is to provide the amount of seepage of liquid water into repository emplacement drifts for TSPA simulations. The emplacement drifts are located in the unsaturated zone at Yucca Mountain, cutting across three geohydrologic units, the Topopah Spring middle nonlithophysal, lower lithophysal, and lower nonlithophysal units. In UZ flow modeling these units are referred to as tsw34, tsw35, and tws36, respectively. These units are all densely welded, highly fractured tuff. In Section 6.2 the basic results from the Seepage Model for PA are summarized and probability distributions that represent the uncertainty and spatial variability of seepage are derived. The basic seepage model is idealized in several respects, including assumptions of no degradation of the drift and no repository thermal effects. In Section 6.3 adjustments to the basic results to take into account several perturbing physical processes are discussed. The adjustments are based on basic physical arguments and on perturbed seepage simulations (CRWMS M&O 2000a, Sections 6.6.4, 6.6.5, 6.6.7). Section 6.4 then presents the final abstraction of seepage that is to be used for TSPA simulations for the Site Recommendation and Section 6.5 discusses the validity of the seepage abstraction for TSPA simulations.

6.2 INITIAL ABSTRACTION OF SEEPAGE RESULTS

6.2.1 Seepage Statistics

Tsang and Li present seepage results for a large number of cases (CRWMS M&O 2000a, Tables 4–8). The tables of results from their report are in the TDMS (see Table 2, item 1). The basic results are for the *seepage percentage* (percentage of percolating water above the footprint of a drift segment that seeps into the drift) for a matrix of values of key input variables. Note that the computed seepage percentage conservatively includes water that seeps into the drift from anywhere on the drift wall; it is not limited to water that seeps in above the footprint of a waste package or drip shield, or even to the top half of the drift (though the amount of water that seeps into the lower half of the drift is small, so including water only from above the springlines would not change the results very much).

The key parameters varied in their simulations are percolation flux above the drift q (denoted Q_p in CRWMS M&O 2000a), the geometric mean of fracture permeability $\bar{k}$ (denoted k_{FC} in CRWMS M&O 2000a), the standard deviation of natural log of permeability σ, and the van Genuchten α parameter (air-entry parameter) for the fractures. Additional information on the parameters and why they are important to seepage can be found in the model report (CRWMS M&O 2000a, Section 6.3). Note that only fracture permeability is heterogeneous in the simulations; α and other parameters have fixed values for each simulation. Computed seepage percentage is available for the following parameter values:

- q = 5, 14.6, 73.2, 213, and 500 mm/yr.
- $\bar{k}$ = 0.9×10^{-14}, 0.9×10^{-13}, 0.9×10^{-12}, and 0.9×10^{-11} m^2.
- σ = 1.66, 1.93, and 2.5 (dimensionless).
- $1/\alpha$ = 30, 100, 300, and 1000 Pa.

Seepage percentage was calculated three times for each combination of the above parameters, with three different geostatistical realizations of the heterogeneity. This is a total of 720 three-dimensional drift-scale flow simulations. Each simulation is for a drift segment slightly longer than a waste package, so the statistics represent the variability and uncertainty of seepage for a single waste-package location. Convergence problems were encountered in some of the seepage simulations. Some simulations are marked in the tables with the note "Steady-state not quite reached (flow out/flow in ≥ 95%)." The seepage percentage listed is used for those cases; it is expected to be within a few percent of the final steady-state value. Other simulations are marked with asterisks in the tables and the note "Seepage large, solution not convergent." For this analysis/model, the seepage percentage is taken to be 100 for those cases (see Section 5, assumption 5).

Examination of the results reveals two characteristics that can be used to simplify the statistical analysis and abstraction: (1) Seepage percentage is not strongly dependent on σ within the range considered. Thus, for the abstraction analysis/model, simulations with all values of σ are lumped together and treated as having nine simulations for each combination of the other parameters. (2) Seepage percentages for simulations with the same value of $\bar{k}/\alpha$—and common values of other parameters—are similar. (They are not reproduced in this report, but Sheet "Seep plots" of the Excel spreadsheet Seep-sr.xls contains plots showing this comparison. The agreement is generally quite good at lower percolation fluxes, and not as good for high percolation fluxes. At the highest end, the spread of seepage percentages is as much as 25% for the simulations with a common value of $\bar{k}/\alpha$.) Thus, for the abstraction analysis/model, seepage is treated as a function of $\bar{k}/\alpha$ rather than of $\bar{k}$ and α separately. With these simplifications, seepage can be treated as a function of just two variables rather than four.

Summary statistical data on seepage percentage for the simulated values of q and $\bar{k}/\alpha$ are given in Table 3. The symbol f_s is used to denote the *seepage fraction*, which is the fraction of waste-package locations (model simulations) that have seepage (i.e., that have nonzero seepage percentage). Note that seepage percentage and seepage fraction are quite different quantities and are not just related by a factor of 100. In calculating the mean values of seepage fraction, seepage percentage, and square of seepage percentage, the mean is a simple average of all simulations with the given values of q and $\bar{k}/\alpha$. For the highest and lowest values of $\bar{k}/\alpha$, the average is over nine simulations (three values of σ times three geostatistical realizations); for the other values of $\bar{k}/\alpha$, the average is over 18 simulations (three values of σ times three geostatistical realizations times two combinations of $\bar{k}$ and α with the given $\bar{k}/\alpha$). For example, $\bar{k}/\alpha = 2.7 \times 10^{-13}$ only occurs for $\bar{k} = 0.9 \times 10^{-14}$ and $1/\alpha = 30$, but $\bar{k}/\alpha = 2.7 \times 10^{-12}$ occurs for $\bar{k} = 0.9 \times 10^{-14}$ and $1/\alpha = 300$ as well as $\bar{k} = 0.9 \times 10^{-13}$ and $1/\alpha = 30$. Note that in the right-most two columns of Table 3 there is an anomalous inversion, with the mean and mean square seepage percentage higher for $\bar{k}/\alpha = 9.0 \times 10^{-13}$ than for $\bar{k}/\alpha = 2.7 \times 10^{-13}$. This anomaly results from many simulations with non-convergent seepage results. As explained above and in Section 5, assumption 5, seepage percentage is conservatively taken to be 100 for non-convergent simulations. We can infer from the inversion in Table 3 that the seepage for $\bar{k}/\alpha = 9.0 \times 10^{-13}$ is somewhat higher than it should be because of this assumption. Since the effect is conservative, it will simply be carried through the subsequent analysis. The actual effect on the final results is not large.

Table 4 gives the same statistical information for *seep flow rate*, which will be denoted Q_s^*. Seep flow rate is defined as the volumetric flow rate of the seepage in a drift segment. The mean seep flow rate is obtained from the mean seepage percentage by multiplying by percolation flux and area; the mean square seep flow rate is obtained from the mean square seepage percentage by multiplying by the square of percolation flux times the square of the area. The area to multiply by is the width of a drift (5.5 m) and the length of an average waste package plus waste-package spacing (5.13 m + 0.1 m), or 28.8 m^2. (Drift diameter, average waste-package length, and waste-package spacing are taken from the TDMS; see Table 2, item 2.) The asterisk is present to indicate that the average is over all seepage simulations. Later, Q_s without an asterisk will be used to indicate the average seep flow rate, averaged over only the simulations that have some seepage (that is, the mean seep flow rate for the locations with seepage). Note that the same anomaly is present in the right-most two columns of Table 4 as in Table 3.

Table 3. Summary Statistical Information for Computed Seepage Percentage

	q = 5 mm/yr			q = 14.6 mm/yr			q = 73.2 mm/yr			q = 213 mm/yr			q = 500 mm/yr		
$\bar{k}/\alpha$	Mean f_s	Mean of Seep %	Mean Square of Seep %	Mean f_s	Mean of Seep %	Mean Square of Seep %	Mean f_s	Mean of Seep %	Mean Square of Seep %	Mean f_s	Mean of Seep %	Mean Square of Seep %	Mean f_s	Mean of Seep %	Mean Square of Seep %
2.7×10^{-13}	1	35.44	1262.78	1	63.22	4007.44	1	85.11	7275.56	1	95.78	9195.78	1	97.44	9509.00
9.0×10^{-13}	1	7.01	54.59	1	36.78	1360.33	1	75.56	5792.67	1	89.67	8095.89	1	99.11	9829.33
2.7×10^{-12}	0.11	0.15	0.38	1	7.77	65.36	1	51.83	2705.94	1	76.00	5866.22	1	89.39	8071.61
9.0×10^{-12}	0	0	0	0.11	0.12	0.25	1	19.39	393.72	1	55.00	3176.44	1	78.00	6289.00
2.7×10^{-11}	0	0	0	0	0	0	0.67	0.91	3.31	1	16.06	261.83	1	41.17	1710.94
9.0×10^{-11}	0	0	0	0	0	0	0	0	0	0.22	0.60	2.36	1	8.94	89.61
2.7×10^{-10}	0	0	0	0	0	0	0	0	0	0	0	0	0.11	0.13	0.32
9.0×10^{-10}	0	0	0	0	0	0	0	0	0	0	0	0	0	0	0
2.7×10^{-09}	0	0	0	0	0	0	0	0	0	0	0	0	0	0	0
9.0×10^{-09}	0	0	0	0	0	0	0	0	0	0	0	0	0	0	0

Input data: see Table 2, item 1. Averages computed in Excel spreadsheet Seep-sr.xls, submitted with this report under DTN: SN9912T0511599.002.

Table 4. Summary Statistical Information for Seep Flow Rate (in m^3/yr)

	q = 5 mm/yr		q = 14.6 mm/yr		q = 73.2 mm/yr		q = 213 mm/yr		q = 500 mm/yr	
$\bar{k}/\alpha$	Mean Q_s^*	Mean Square Q_s^*	Mean Q_s^*	Mean Square Q_s^*	Mean Q_s^*	Mean Square Q_s^*	Mean Q_s^*	Mean Square Q_s^*	Mean Q_s^*	Mean Square Q_s^*
2.7×10^{-13}	5.10×10^{-2}	2.61×10^{-3}	0.266	7.07×10^{-2}	1.79	3.23	5.87	34.5	14.0	197
9.0×10^{-13}	1.01×10^{-2}	1.13×10^{-4}	0.154	2.40×10^{-2}	1.59	2.57	5.49	30.4	14.3	203
2.7×10^{-12}	2.09×10^{-4}	7.77×10^{-7}	3.26×10^{-2}	1.15×10^{-3}	1.09	1.20	4.66	22.0	12.9	167
9.0×10^{-12}	0	0	5.18×10^{-4}	4.34×10^{-6}	0.408	0.175	3.37	11.9	11.2	130
2.7×10^{-11}	0	0	0	0	1.91×10^{-2}	1.47×10^{-3}	0.984	0.983	5.92	35.4
9.0×10^{-11}	0	0	0	0	0	0	3.70×10^{-2}	8.86×10^{-3}	1.29	1.85
2.7×10^{-10}	0	0	0	0	0	0	0	0	1.93×10^{-2}	6.62×10^{-3}
9.0×10^{-10}	0	0	0	0	0	0	0	0	0	0
2.7×10^{-09}	0	0	0	0	0	0	0	0	0	0
9.0×10^{-09}	0	0	0	0	0	0	0	0	0	0

Numbers from Table 3 converted in Excel spreadsheet Seep-sr.xls, submitted with this report under DTN: SN9912T0511599.002.

6.2.2 Spatial Variability of k/α

The next step in the analysis is to assign probabilities, or weights, to the various cases in Table 3 and Table 4. There is a fair amount of permeability data available from air-injection tests. However, only a small subset of the data relates to characterization of the disturbed zone around the emplacement drifts, where the fracture properties are altered by the excavation. The properties of this disturbed zone are more relevant to calculations of seepage than properties of undisturbed rock, since the zone immediately surrounding the drifts is where the processes that determine seepage take place. Pre- and post-excavation data from three niches in the ESF are discussed in an analysis report (CRWMS M&O 2000c, Section 6.1); summary numbers are in the TDMS (see Table 2, item 3). The post-excavation data from these niches are the best data available for determining the permeability field in the disturbed zone around an emplacement drift. The shape is not the same, but the width and height of the niches are comparable to emplacement drifts (approximately 4 m × 3 m, whereas emplacement drifts are to be 5.5-m-diameter circles), so the geometric-average measured post-excavation permeability should be a reasonable analog for $\bar{k}$, which is the geometric average of the permeability field in the seepage model. The data and averages are given in Table 5.

Table 5. Niche Air-Permeability Data

	Mean log(k) (k in m^2)	Std.Dev. log(k) (k in m^2)	Std.Dev. ln(k) (k in m^2)
Niche 3650	–11.8	0.88	2.0
Niche 3107	–12.4	0.82	1.9
Niche 4788	–11.9	0.78	1.8
Mean	**–12.03**	0.83	1.9
Std.Dev.	**0.32**	0.050	0.12

Input data: Table 2, item 3. Averages computed in Excel spreadsheet Seep-sr.xls, submitted with this report under DTN: SN9912T0511599.002.

Based on this information, a log-normal distribution will be used for $\bar{k}$, with log mean of –12.03 and log standard deviation of 0.32. Note the distinction between the standard deviation of mean log(k), which is in the second column of the table, and the mean of the standard deviation of log(k), which is in the third column of the table. The values listed for mean log(k) are direct analogs of log($\bar{k}$) at different locations. Their mean and standard deviation, then, represent the variability of mean disturbed-zone permeability from location to location. The values listed for standard deviation of log(k), on the other hand, represent the smaller-scale variability of disturbed-zone permeability at a particular location, which is parameterized by σ in the seepage model. Note, however, that the σ parameter is defined to be a natural log. Natural-log values are given in the last column of Table 5, and their mean and standard deviation could be used to define a distribution for σ if it were needed. A potentially important limitation of these data is that they all come from the Topopah Spring middle nonlithophysal unit. No comparable data are available from the other repository host units (Topopah Spring lower lithophysal and lower nonlithophysal). This lack of data will be discussed again in Section 6.2.3. Note that the

disturbed-zone fracture properties are applied to the entire model domain, including the region beyond the disturbed zone, in the seepage simulations. This approach is discussed in the model reports (CRWMS M&O 2000d, Sections 5.3.5 and 6.3.2; CRWMS M&O 2000a, Section 6.3.2).

Next we need information on the van Genuchten α parameter for fractures. There is very little direct information on this parameter. It is typically estimated by means of theoretical formulations, such as the "cubic law" for fracture permeability as a function of aperture (see, for example, Bodvarsson et al. 1997, Sections 7.5.4 and 7.5.5). There is only one known value of α that is based on actual water-flow data, from the Finsterle and Trautz calibration of seepage tests at Niche 3650 in the ESF (CRWMS M&O 2000d, Section 6.4). Their best-estimate value for a three-dimensional heterogeneous conceptual model (which is the conceptual model used in the Seepage Model for PA, including the convention that disturbed-zone properties are used throughout the entire model domain) is $\log(1/\alpha) = 1.82$ ($1/\alpha$ in Pa), or $1/\alpha = 66$ Pa (CRWMS M&O 2000d, Table 10; also see Table 2 of this report, item 4). This leads to a best-estimate value of $\log(\bar{k}/\alpha) = -12.03 + 1.82 = -10.21$, or $\bar{k}/\alpha = 6 \times 10^{-11}$ m^2·Pa. (Note that the value of $\bar{k}$ in the calibration of α was 2.2×10^{-12} m^2, so $\bar{k}/\alpha$ for the Niche-3650 tests was determined to be about 14.5×10^{-11} m^2·Pa.)

There are no data on the spatial distribution or standard deviation of α. Theoretically, it is believed that α and k are correlated because they are both related to fracture aperture. Sometimes they are even taken to be perfectly correlated (CRWMS M&O 2000d, Section 6.3.2; CRWMS M&O 2000a, Section 6.3.4). Correlation is important because the standard deviation of $\bar{k}/\alpha$, which is needed for the abstraction analysis/model, is related to the standard deviations of $\bar{k}$ and α by $\sigma^2_{\log(k/\alpha)} = \sigma^2_{\log(k)} + \sigma^2_{\log(\alpha)} - 2c\sigma_{\log(k)}\sigma_{\log(\alpha)}$, where c is the correlation coefficient. In order to estimate an appropriate standard deviation for $\log(\bar{k}/\alpha)$, suppose for the moment that $\alpha = \bar{k}^{1/n}$. Then $\sigma_{\log(\alpha)} = \frac{1}{n}\sigma_{\log(k)}$ and

$$\sigma^2_{\log(k/\alpha)} = (1 + \frac{1}{n^2} - \frac{2c}{n})\sigma^2_{\log(k)} \qquad \text{(Eq. 1)}$$

The relation used in the Seepage Calibration Model (CRWMS M&O 2000d, Section 6.3.2) corresponds to n = 2 and $c = 1$; the "cubic law" for fracture permeability corresponds to n = 3. The quantity $\mathrm{sqrt}(1 + \frac{1}{n^2} - \frac{2c}{n})$ is listed in Table 6 for n equal to 2 and 3 and c from 0 to 1. The range of values is fairly small—only from 0.5 to 1.12. Since there is no information on the correct value for $\sigma_{\log(k/\alpha)}$, and the estimates implied by the values in Table 6 do not cover a very large range, we will opt for the simplicity of setting $\sigma_{\log(k/\alpha)} = \sigma_{\log(k)}$. This assumption is only used for estimating the spatial variability of $\bar{k}/\alpha$ and, in consequence, the spatial variability of seepage. A wider range of assumptions about $\bar{k}/\alpha$ is taken into account by means of an uncertainty distribution, which will be discussed in Section 6.2.3.

Table 6. Ratio of Std.Dev. $\bar{k}/\alpha$ to Std.Dev. $\bar{k}$

n	*c*		
	0	**0.5**	**1**
2	1.12	0.87	0.50
3	1.05	0.88	0.67

Calculated using Eq. 1 in Excel spreadsheet Seep-sr.xls, submitted with this report under DTN: SN9912T0511599.002.

In Section 6.2.4, $\sigma_{\log(k/\alpha)}$ will be used to define weighting factors that are used to combine seepage results for multiple $\bar{k}/\alpha$ cases into a single weighted estimate of seepage for a given percolation flux. That is, each value in Table 8 is a weighted combination of seepage results for several $\bar{k}/\alpha$ values in Table 4. Larger $\sigma_{\log(k/\alpha)}$ would lead to combining more values, while smaller $\sigma_{\log(k/\alpha)}$ would lead to combining fewer values. Because of the nonlinearity of the seepage–$\bar{k}/\alpha$ relationship, especially at lower percolation fluxes, the effect of combining results for multiple $\bar{k}/\alpha$ cases is generally to increase the seepage estimate, because some weight is given to lower $\bar{k}/\alpha$, where seepage can be much higher. Thus, using $\sigma_{\log(k/\alpha)} = \sigma_{\log(k)}$ is conservative compared to using the lower values implied by higher correlations (for example, $\sigma_{\log(k/\alpha)} = 0.5\ \sigma_{\log(k)}$ if $n = 2$ and $c = 1$).

6.2.3 Uncertainty in k/α

The distinction between spatial variability and uncertainty in $\bar{k}/\alpha$ (or any other parameter) can be understood in terms of the way a TSPA calculation works. A TSPA calculation is a Monte Carlo simulation, in which a number of realizations of the total system are generated and repository performance computed for each one. The Monte Carlo simulation is basically an uncertainty analysis: Each realization is normally taken to be equally likely, so any one of the realizations could be the "correct" one. The differences between one realization and another are within the range of our uncertainty about each parameter that is varied. Some parameters, like fracture permeability or α parameter, are uncertain, so they vary from one TSPA realization to another, but they are also spatially variable, so they vary from location to location within each TSPA realization.

The spatial variability of the combination $\bar{k}/\alpha$ was discussed in Section 6.2.2. As has already been discussed, there is only one relevant calibrated value of α, so it is highly uncertain. There are several measurements of the geometric-mean permeability, $\bar{k}$, within the Topopah Spring middle nonlithophysal unit, so it can be regarded as reasonably well characterized for that unit, but the appropriate values for the other repository host units have to be considered uncertain. Thus, in addition to spatial variability within each TSPA realization, it is important to treat $\bar{k}/\alpha$ as uncertain and vary it across realizations.

With few data available, the treatment of uncertainty is necessarily somewhat arbitrary. One source of information that can help guide the choice is the calibrated properties for the site-scale UZ flow model. In addition to the site-scale properties, a set of properties for drift-scale models

was also developed, the only difference being the fracture permeability for some of the layers. (CRWMS M&O 2000e, Tables 13–15 and 17; DTNs: LB990861233129.001, LB990861233129.002, and LB990861233129.003). The drift-scale values of fracture permeability for the repository units (tsw34 through tsw36 in the terminology of CRWMS M&O 2000e) range from 2.76×10^{-13} to 5.09×10^{-12} m^2, which is within the range of values being used for seepage simulations. On the other hand, the values of fracture α for the repository units range from 2.48×10^{-4} to 9.43×10^{-4} Pa^{-1}, which correspond to $1/\alpha$ values (1060 to 4030 Pa) that are higher than the values being used for seepage simulations. The resulting k/α combinations range from 5.35×10^{-10} to 5.40×10^{-9} $m^2 \cdot Pa$, all much higher than the estimate above of 6×10^{-11} $m^2 \cdot Pa$ for seepage. In addition, the drift-scale k/α values for the other host units (tsw35 and tsw36) are higher than for the middle nonlithophysal unit (tsw34) for every infiltration case.

These bits of information all point toward higher values of k/α, which is of interest because, as can be seen in Table 3 and Table 4, higher values of k/α indicate less seepage. To account for the uncertainty, a range of values will be considered. The available information indicates that our uncertainty is more toward higher values of $\bar{k}/\alpha$, so the range considered will be skewed somewhat to higher values: Values of $\bar{k}/\alpha$ from one-half order of magnitude lower to one order of magnitude higher than 6×10^{-11} $m^2 \cdot Pa$ will be considered. This is the range of values for the geometric mean of the distribution of $\bar{k}/\alpha$ from location to location; in each case the standard deviation of the distribution of $\log(\bar{k}/\alpha)$ from location to location will be taken to be 0.32 (see Table 5).

6.2.4 Variability and Uncertainty of Seepage

Given a distribution for $\bar{k}/\alpha$, a corresponding distribution can be developed for seepage using the information in Table 3 and Table 4. To do that, the $\bar{k}/\alpha$ distribution must first be discretized—that is, the continuous distribution must be converted to discrete weighting factors for the $\bar{k}/\alpha$ values in Table 3 and Table 4. The weighting factors are first set equal to the log-normal probability density function at the given values of $\bar{k}/\alpha$, and then they are all divided by a normalization factor chosen to make the weights add up to 1. This process is illustrated in Table 7 for the best-estimate case where the distribution is centered at $\log(\bar{k}/\alpha) = -10.21$. (Recall that the best-estimate case is based on air-permeability and seepage tests in the Topopah Spring middle nonlithophysal unit.) To simplify the subsequent seepage analysis, weighting factors less than 10^{-3} are truncated to zero (that is, the ones not bold in the table). The result of this simplification is just that some seepage estimates in the final abstraction are zero rather than some extremely low value. Such low probabilities and low seepage estimates are below the level that is really supported by the data. The four discrete weighting factors shown in bold in Table 7 reproduce the log-normal distribution quite well, having a mean of –10.21 and a standard deviation of 0.33 (slightly higher than the desired value of 0.32). The same weighting factors can be shifted to the right or left to obtain log-normal distributions for other mean values of $\bar{k}/\alpha$ that are higher or lower by an order of magnitude. For $\bar{k}/\alpha$ one-half order of magnitude lower (or higher), the weighting factors are slightly different, since the $\bar{k}/\alpha$ values available are not

quite evenly spaced. The discrete distribution for that case will not be presented here, but can be found in the spreadsheet Seep-sr.xls.

Table 7. Discrete Log-Normal Distribution of $\bar{k}/\alpha$ for the Best-Estimate Case

$\bar{k}/\alpha$	2.7×10^{-12}	9.0×10^{-12}	2.7×10^{-11}	9.0×10^{-11}	2.7×10^{-10}	9.0×10^{-10}	2.7×10^{-9}
$x = \log(\bar{k}/\alpha)$	–11.57	–11.05	–10.57	–10.05	–9.57	–9.05	–8.57
$\exp\{-(x-\mu)^2/2\sigma^2\}$ $\mu = -10.21$ $\sigma = 0.32$	1.4×10^{-4}	0.035	0.543	0.873	0.134	1.4×10^{-3}	2.1×10^{-6}
Normalized Weight	8.7×10^{-5}	**0.022**	**0.343**	**0.551**	**0.084**	8.6×10^{-4}	1.3×10^{-6}

Taken from Excel spreadsheet Seep-sr.xls, submitted with this report under DTN: SN9912T0511599.002. Note that the spreadsheet does not round off at intermediate steps, whereas the values in this table are rounded.

If the seepage information in Table 3 and Table 4 is combined with the weighting factors in Table 7, weighted seepage statistics are obtained, representing the distribution of spatial variability of seepage within a TSPA realization. Those results are shown in Table 8 for three geometric-mean $\bar{k}/\alpha$ values: the best-estimate value of 6×10^{-11} m^2·Pa, plus geometric-mean values one-half order of magnitude lower and one order of magnitude higher.

Table 8. Weighted Seepage Statistics for the Basic Seepage Results

	Geo.Mean $\bar{k}/\alpha = 2\times10^{-11}$			**Geo.Mean $\bar{k}/\alpha = 6\times10^{-11}$**			**Geo.Mean $\bar{k}/\alpha = 6\times10^{-10}$**		
q (mm/yr)	**f_s**	**Mean of Q_s (m^3/yr)**	**Std.Dev. of Q_s (m^3/yr)**	**f_s**	**Mean of Q_s (m^3/yr)**	**Std.Dev. of Q_s (m^3/yr)**	**f_s**	**Mean of Q_s (m^3/yr)**	**Std.Dev. of Q_s (m^3/yr)**
5	1.97×10^{-3}	1.88×10^{-3}	1.86×10^{-3}	0	0	0	0	0	0
14.6	5.75×10^{-2}	1.33×10^{-2}	1.44×10^{-2}	2.45×10^{-3}	4.66×10^{-3}	4.16×10^{-3}	0	0	0
73.2	0.744	0.237	0.240	0.250	6.22×10^{-2}	0.116	0	0	0
213	0.944	1.94	1.32	0.487	0.887	0.675	4.91×10^{-3}	0.167	0.110
500	0.999	7.61	3.36	0.925	3.23	2.63	6.01×10^{-2}	0.582	0.616

Taken from Excel spreadsheet Seep-sr.xls, submitted with this report under DTN: SN9912T0511599.002.

Calculation of the weighted-mean seepage fraction f_s is straightforward. It is simply given by

$$\langle f_s(q) \rangle = \sum w_i f_s(x_i, q) \qquad \text{(Eq. 2)}$$

where the sum is over the discrete values of $x = \bar{k}/\alpha$ and w_i are the normalized weighting factors in Table 7. Calculation of the weighted mean and standard deviation of Q_s is slightly more complicated because the mean over locations with seepage is desired, rather than the overall mean. For the mean, it is just a matter of adjusting the average by the fraction of locations that have seepage:

$$\langle Q_s(q)\rangle = \frac{\sum w_i Q_s^*(x_i,q)}{\langle f_s(q)\rangle} = \frac{\langle Q_s^*(q)\rangle}{\langle f_s(q)\rangle} \quad \text{(Eq. 3)}$$

In this equation, $\langle Q_s^*(q)\rangle$ is the average seep flow rate over all locations, as listed in Table 4. The division by the seepage fraction makes it into an average over just the locations with seepage. The mean square seep flow rate, adjusted by seepage fraction, is calculated in the same way, and then the standard deviation of seep flow rate is obtained from

$$\sigma_{Q_s}^2 = \langle Q_s^2(q)\rangle - \langle Q_s(q)\rangle^2 \quad \text{(Eq. 4)}$$

The standard deviations of seep flow rate in Table 8 are relatively large: nearly as large as the mean in most cases and even larger than the mean in a few cases. These large standard deviations result from the large differences in seepage from one set of simulations to another. For example, the weighted mean and standard deviation for $\bar{k}/\alpha = 6 \times 10^{-11}$ m^2·Pa are a combination of the results for $\bar{k}/\alpha$ values of 9×10^{-12}, 2.7×10^{-11}, 9×10^{-11}, and 2.7×10^{-10} m^2·Pa (see Table 7). Examination of the summary information in Table 4 shows that over that range of $\bar{k}/\alpha$ values the mean seep flow rate at 73.2 mm/yr goes from zero to 0.408 m^3/yr. Thus, an amount of spatial variability in $\bar{k}/\alpha$ corresponding to a log standard deviation of 0.32 (see Section 6.2.2) translates into a relatively large spatial variability of seepage. This is consistent with the concept of seepage as a random process (see assumption 1 in Section 5).

6.3 ADJUSTMENTS FOR OTHER EFFECTS

6.3.1 Drift Degradation and Rock Bolts

The basic seepage simulations that have been discussed so far were computed assuming the design drift configuration. Degradation of the drifts over time is expected and has been evaluated (CRWMS M&O 1999f). The effect that changes in drift shape might have on seepage is of concern. The Seepage Model for PA report (CRWMS M&O 2000a) includes some discussion of the impacts of drift degradation on seepage in Section 6.4 and results of some seepage simulations with degraded drift shapes in Section 6.6.5. A total of nine degraded-drift seepage simulations were performed (CRWMS M&O 2000a, Table 12; also see Table 2 of this report, item 1). Degraded drift shapes lead to increases in computed seepage, with the increase ranging from negligible to 90% for the worst case modeled. (The three geostatistical realizations for that case had seepage increases of approximately 30%, 90%, and 45%, for an average increase of about 55%.) It is proposed (CRWMS M&O 2000a, Section 6.6.5) that the increase in seepage is approximately proportional to the increase in drift-wall area (including voids from which blocks have fallen in the area calculation). This approximation could be used to estimate seepage for cases that have not been computed with the seepage model.

The worst cases reported in the drift-degradation analysis (CRWMS M&O 1999f, Section 6.4.3) have worse drift degradation than the cases for which seepage is modeled (CRWMS M&O 2000a, Sections 6.4 and 6.6.5). However, the drift-degradation results indicate that the rock in the repository is strong enough that drift failures are infrequent: The fraction of drift length affected by rockfall ranges from only 1.1% up to 12.9% for the repository host units (CRWMS

M&O 1999f, Figures 32–34). Furthermore, the lowest number (1.1%) is for the host unit that contains most of the repository (Topopah Spring lower lithophysal). While we want to increase the seepage amounts to account for drift degradation, it would greatly overestimate the effects to assume the worst possible degradation at all locations.

An additional consideration is the possibility that the rock bolts used for ground support could become preferential paths for seepage as they degrade. This "surface needle" effect could be important (CRWMS M&O 2000a, Sections 6.7 and 7). According to a preliminary estimate, seepage could increase by as much as 70%, depending on how many of these preferential paths there are. Specifically, increases of 3%, 40%, and 70% are reported for cases with 3, 33, and 330 "needles" along a 16.5-m length of drift (CRWMS M&O 2000a, Section 6.7). According to a design input transmittal (CRWMS M&O 1999g), rock bolts are not planned for the lower lithophysal unit, which will contain most of the repository, but in the nonlithophysal units there may be six rock bolts every 1.5 m along the drifts, which would be 66 along a 16.5-m length of drift. Thus, the preliminary estimate would be for an increase of somewhat more than 40% due to the rock bolts in the nonlithophysal units.

To summarize, a potential for increased seepage is indicated in locations where rock bolts are used for ground support, which is expected to be principally in the nonlithophysal repository host units. In addition, after the ground support has degraded and the shape of the drifts starts to degrade, the seepage model predicts increased seepage. The potential for drift degradation is predicted to be higher in the nonlithophysal units than in lithophysal rock, and highest in the middle nonlithophysal unit. The effects of rock bolts and drift degradation on seepage are not necessarily additive, however. In locations where drift degradation is minor, the rock-bolt effect would dominate, and in locations with extensive drift degradation the damage can extend above the rock-bolt holes, so they no longer have an additional effect. As just discussed, the potential for both of these effects is lower in the lower lithophysal unit, where most of the emplacement drifts are to be located. However, because of the uncertainty associated with these effects, and because we wish to simplify the treatment of seepage in the TSPA, the lower lithophysal unit will conservatively not be differentiated from the others in the abstraction.

As an approximate treatment, seepage will be increased by the average of the increase for the worst case considered in the process modeling (CRWMS M&O 2000a, Section 6.6.5). That is, for TSPA the seep flow rates in Table 8 will be increased by 55% as an adjustment for drift degradation and rock bolts. According to the drift-degradation analysis, there is only a small probability of more extensive drift degradation (the most extreme cases in Figures 32–34 of CRWMS M&O 1999f). And according to the preliminary evaluation of rock-bolt effects on seepage, they would only increase seepage by more than 55% if very large numbers of rock bolts were used.

6.3.2 Possible Correlation of α and k

As discussed above in Section 6.2.2, there are theoretical reasons to expect fracture permeability and the fracture α parameter to be correlated. The discussion in Section 6.2.2 was concerned with correlation between their average values, but correlation within the model domain is also a possibility. The Seepage Calibration Model treated α and k as perfectly correlated (CRWMS M&O 2000d, Section 6.3.2), but the Seepage Model for PA simplified the model by treating α as

a constant for each simulation (CRWMS M&O 2000a, Section 6.3.4). A limited number of cases were run with correlation between α and k, for comparison; the seepage results were quite similar, but higher by up to 10%. Since the true amount of correlation between α and k is unknown, for TSPA we will be conservative and increase the seep flow rates in Table 8 by 10% as an adjustment for this possible effect.

6.3.3 Focusing of Flow above the Drifts

Focusing of flow in the unsaturated zone is an issue for seepage into drifts, since it could result in higher fluxes in some locations, which would then increase the amount of seepage in those locations. Flow focusing on large scales (hundreds of meters) is taken into account by the site-scale UZ flow model (e.g., Bodvarsson et al. 1997, Chapter 20). Flow focusing on small scales (a few meters) is already included in the drift-scale UZ flow model that is used for seepage calculations (CRWMS M&O 2000a). What is missing is an explicit consideration of flow focusing on intermediate scales (tens of meters). Such focusing could potentially concentrate flow from an area of tens of meters square onto a particular drift segment, thereby increasing the local percolation flux and seepage at that location. It is important to realize, though, that if flow is concentrated in one location, conservation of water mass requires that flow be reduced in other areas so that the total amount of water flow is unchanged.

The "active fracture" conceptual flow model (Liu et al. 1998) that is being used for site-scale UZ flow calculations is based on the concept that flow is channeled in fractures, so that only some fractures are actively flowing. This conceptual model can provide an estimate of the degree of channeling in fractures and thus the degree of intermediate-scale focusing of flow.

6.3.3.1 Calculation of Weep Spacings

Discrete fracture flow paths, referred to as "weeps," are believed to occur in the unsaturated zone at Yucca Mountain as a result of heterogeneities and instabilities in wetting-front propagation. While channeling and fingering of flow have been observed in laboratory settings (Glass and Tidwell 1991, p. 50), current models of flow through the UZ at Yucca Mountain are based on continuum approximations. In this analysis/model, the weep spacing is calculated as the distance that separates the active fractures, which is typically larger than the geometric spacing of fractures used in the development of the continuum model. The weep spacings can be derived from dual-continuum models as described in Ho and Wilson (1998) and Liu et al. (1998). A slightly modified version of the method used in Ho and Wilson (1998) is presented here to derive an upper bound for the weep spacings assuming that each active fracture is saturated (i.e., flow occupies the entire fracture). The method used in Liu et al. (1998, Section 2.4) assumes that the active fractures are unsaturated, and Eq. 17 in that paper is used to provide a lower bound on the weep spacings.

Upper Bound on Weep Spacings. The upper bound on weep spacing is calculated using geometric arguments for the reduced wetted fracture area in a computational grid block of the site-scale UZ flow model. In Ho and Wilson (1998), the ratio of the available weep area, A_{weep}, to the total geometric fracture area, A_{DKM}, in a computational grid block was defined as a fracture/matrix reduction factor, X_{fm}:

$$X_{fm} = \frac{A_{weep}}{A_{DKM}} \quad \text{(Eq. 5)}$$

In the site-scale flow fields, the geometric fracture area, A_{DKM}, per volume of grid block, V, is provided as a constant parameter ($A^* = A_{DKM}/V$) for each unit. The available weep area, A_{weep}, is derived in this analysis/model assuming that each fracture containing a weep is saturated. This is equivalent to assuming that the weep width w is equal to the weep spacing a in Eq. 3 of Ho and Wilson (1998), yielding $A_{weep} = 2V/a$. Substituting these relations into Eq. 5 and solving for the weep spacing yields:

$$a = \frac{2}{X_{fm} A^*} \quad \text{(Eq. 6)}$$

To be consistent with the active-fracture model used in the site-scale flow fields, the reduction factor X_{fm} is calculated as the product of the first two terms on the right-hand side of Eq. 12 of Liu et al. (1998), which describes the ratio of the available weep area to the total fracture area per grid block. The resulting reduction factor X_{fm} is equal to the effective liquid saturation, S_e, of the fractures in the grid block:

$$X_{fm} = S_e = \frac{S_f - S_r}{1 - S_r} \quad \text{(Eq. 7)}$$

where S_f is the average liquid saturation of the fractures in the grid block and S_r is the residual liquid saturation of the fractures. Eqs. 6 and 7 yield an upper bound to the discrete weep spacings because the active fractures are assumed to be saturated, which maximizes the distances separating the active fractures.

Lower Bound on Weep Spacings. Eq. 17 from Liu et al. (1998) is used directly to calculate a lower bound for the weep spacing a (i.e., the separation distance between active fractures):

$$a = \frac{d}{S_e^{\gamma}} \quad \text{(Eq. 8)}$$

where d is the geometric fracture spacing for each grid block (constant for each unit) and γ is a calibrated parameter (between 0 and 1) that is associated with the fraction of fractures that are active in the fracture network. The active fractures are assumed to be unsaturated, so the derived spacing in Eq. 8 will be less than if the active fractures are assumed to be saturated as given in Eqs. 6 and 7.

The parameters used in Eqs. 6–8 that are relevant to this analysis/model are summarized in Table 9. Note that tswF4, tswF5, and tswF6 refer to the fracture materials in the Topopah Spring middle nonlithophysal, lower lithophysal, and lower nonlithophysal units, respectively; tswFf refers to the fracture material in fault zones.

Table 9. Hydrologic Parameters Used in Calculation of Weep Spacings

Material	A^* (m^2/m^3)	d (m)	S_r	γ		
				Low Infiltration	Base Infiltration	High Infiltration
tswF4	13.54	0.23	0.01	0.23	0.41	0.38
tswF5	9.68	0.32	0.01	0.23	0.41	0.38
tswF6	12.31	0.25	0.01	0.23	0.41	0.38
tswFf	8.6	0.59	0.01	0.5	0.5	0.5

A^*, d inputs: see Table 2, item 12; S_r, γ inputs: see Table 2, items 5–7.

Results. A software routine, T2WEEP v. 1.0, was written to calculate the weep spacings derived above. The steps that T2WEEP performs are summarized as follows:

1) Read in user-prescribed files and data.
2) Read in repository elements from user-prescribed file.
3) Read in element information (name, material, coordinates) from ELEME card and assign parameter values to repository elements.
4) Read in connection information from CONNE card for connections between repository element and element directly above it. Record connection area.
5) Read TOUGH2 output file. First read in liquid saturations for prescribed repository elements. Then read in mass flow rates for repository connections.
6) Calculate percolation flux (not used in weep-spacing calculation) from mass flow using connection area and liquid density.
7) Calculate weep spacing using Eqs. 6–8.
8) Print results to output file.

In addition to the input values listed in Table 9, inputs are site-scale UZ flow fields and mesh file. Attachment I provides sample input and output files for T2WEEP, as well as the listing of the source file. The sample files in Attachment I constitute a test case for the routine. Values for the calculated percolation flux and weep spacings were spot-checked in the sample output file to ensure that the software routine was performing correctly. Results were verified in this manner for the input and output files used in this analysis. Thus, the range of input parameter values for which results were verified are those listed in Table 9, plus the particular UZ flow fields discussed below.

All input and output files used in the T2WEEP calculations have been submitted to the TDMS under DTN: SN9912T0511599.002. Note that in Attachment I and in the files submitted to the TDMS the mesh file is referred to as mpa_pch1.v1. This is the name as it was originally received in an input transmittal. In the final submission to the TDMS (see Table 2, item 11) the name of the file was changed to 3d2kpa_pc1.mesh. It was confirmed through a UNIX "diff" command that the two are, indeed, the same.

In order to calculate the weep spacings, elements must be prescribed so that relevant hydrologic parameters and variables are appropriately assigned. Attachment II contains a description and listing of the elements that are used to derive the weep spacing of flow entering the repository region. The repository outline is taken from the TDMS (see Table 2, item 13).

A number of flow fields have been generated for the TSPA for Site Recommendation, including flow for three climate states (present-day, monsoon, and glacial transition), three infiltration levels (low, "base," and high), and two alternative models for flow beneath the repository (perched-water models #1 and #2). The percolation fluxes and liquid saturations at the repository horizon are not affected by the different perched-water models, so only model #1 is used. The glacial-transition climate is chosen to obtain the weep-spacing distributions because that climate is in effect most of the time; the present-day and monsoon climates are only in effect at relatively early times. Thus, T2WEEP is run for three flow fields: (1) glacial-transition climate, low infiltration, perched-water model #1; (2) glacial-transition climate, base infiltration, perched-water model #1; and (3) glacial-transition climate, high infiltration, perched-water model #1 (see Table 2, items 8–10).

Results for the base-infiltration case are shown in Figure 1. (Results for the other two cases are qualitatively similar.) Shown are histograms for the log of weep spacing assuming saturated active fractures (Eqs. 6–7) and unsaturated active fractures (Eq. 8). Note that the repository elements that were assigned fault properties (as denoted by an 'f' in the fifth character of the material name) have been excluded from the histograms. The elements with fault properties used parameters significantly different from the other repository units (see Table 9) and yielded extremely large weep spacings that could exceed the size of the grid block. It makes sense to exclude the fault elements from this analysis because we are concerned with seepage at waste-package locations, and waste packages are not expected to be emplaced directly in fault zones. It can be seen in the figure that both methods produce weep spacings that are approximately log-normally distributed and that, as expected, the assumption of saturated active fractures leads to larger weep-spacing estimates. The means and standard deviations of log spacings are listed in Table 10.

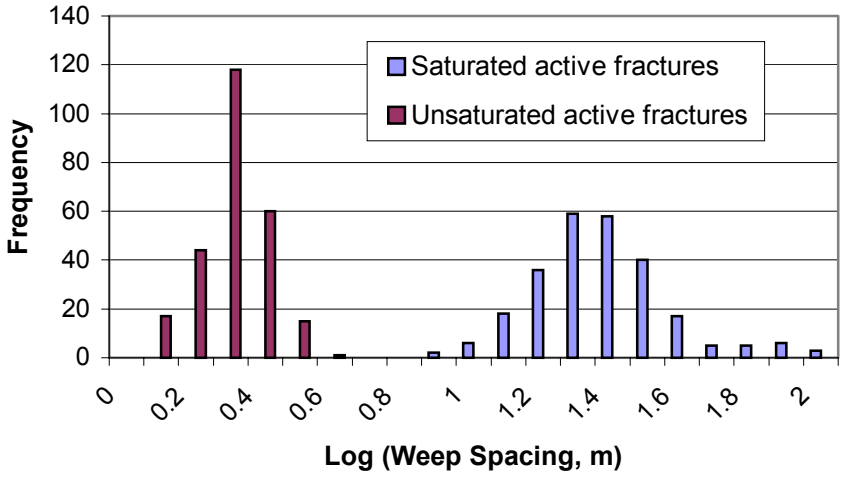

Figure 1. Histograms of Log Weep Spacing for Glacial-Transition Climate and Base Infiltration

Taken from Excel spreadsheet Seep-sr.xls, submitted with this report under DTN: SN9912T0511599.002.

Table 10. Statistics for Weep Spacings, Glacial-Transition Climate

		Low Infiltration	Base Infiltration	High Infiltration
Log(*a*) (saturated active fractures; *a* in m)	**Mean**	1.43	1.43	1.23
	Std.Dev.	0.35	0.19	0.21
Log(*a*) (unsaturated active fractures; *a* in m)	**Mean**	–0.03	0.36	0.22
	Std.Dev.	0.11	0.10	0.10

Taken from Excel spreadsheet Seep-sr.xls, submitted with this report under DTN: SN9912T0511599.002.

Note that the spacings tend to increase with lower infiltration. The reduced infiltration reduces the number of actively flowing fractures, which consequently increases the weep spacing. The weep spacings for low infiltration do not fit smoothly on the trend for the two higher-infiltration cases because the active-fracture γ parameter is significantly different for low infiltration (see Table 9).

6.3.3.2 Distribution of Flow-Focusing Factors

The mean log spacing of 1.43 for the base-infiltration case (see Table 10) corresponds to an actual spacing of about 27 m. A spacing of 27 m between flowing fractures would indicate a potential for the flow from a 27 m × 27 m area to be focused into a relatively small area. This is the estimate based on saturated flowing fractures in the active-fracture model (see Section 6.3.3.1 and Eqs. 6 and 7). The estimate based on unsaturated flowing fractures is much smaller—only 2.3 m (see Table 10).

The upper-boundary area in the drift seepage model is 15 m × 5.23 m = 78.5 m^2 (CRWMS M&O 2000a, Section 6.3.1). The area corresponding to 27 m × 27 m is 729 m^2. If all the flow from 729 m^2 were focused into the area above one of these model domains, that would lead to a local percolation flux a factor of about 9.3 times as high as the average (729/78.5). On the other hand, spacings of up to several meters are contained within the size of the model, and focusing over that distance would not be expected to change the seepage model significantly. (Note that water flow within a seepage simulation would take place primarily within the high-permeability channels of the heterogeneous model regardless of how flux is introduced at the boundary.) Thus, a range of focusing factors is supported by the information available. The shape of the distribution is speculative, but a log-uniform distribution will be used, as it is appropriate for an uncertain multiplicative factor. The lower bound of the log-uniform distribution should be 1, or no significant focusing. The upper bound will be taken from one standard deviation above the mean of the log weep-spacing distribution. Because of the normal shape of the log weep-spacing distributions (see Figure 1) the likelihood of values higher than one standard deviation above the mean is small, and they would not be appropriate for use with a log-uniform distribution of focusing factors. An example of the derivation of the upper bound is as follows. For the base-infiltration case, the mean and standard deviation of log spacing from Table 10 are 1.43 and 0.19, respectively, so one standard deviation above the mean is at $\log(a) = 1.62$, or $a \cong 42$ m. An area of 42 m × 42 m is about 1800 m^2, and this area divided by 78.5 m^2 (the area of the seepage

model domain) gives a focusing factor of approximately 22, which is used for the upper bound of the log-uniform distribution of focusing factors for base infiltration. In a similar manner, the upper bounds for low and high infiltration are found to be approximately 47 m and 9.7 m, respectively. As noted above, the estimated weep spacings, and thus the estimated focusing factors, are higher when infiltration is lower.

This distribution of flow-focusing factors is an uncertainty distribution, which means that one value of it is sampled for each TSPA realization. That value is then applied to modify the spatial variability of seepage within the realization. The way it would be applied is as follows. Say the initial estimate of percolation flux at a location is q_i and the focusing factor is F. The percolation flux is modified to $q = Fq_i$ and the seepage fraction f_s and seep flow rate Q_s are calculated (or sampled from distributions) based on that flux. They will be higher than if they had been calculated using q_i because q is a higher flux. But further modification is necessary, because a higher flux q over an area implies lower fluxes over a larger area in order to preserve the correct average percolation flux (in other words, in order to conserve water mass). Percolation increased by a factor of F over an area A would have to be balanced by zero flux over an area $(F–1)A$ (or a nonzero flux over an even larger area) in order to leave the average flux unchanged. A simple abstraction for this effect is to reduce the seepage fraction by F to f_s/F, consistent with a conceptual picture that percolation increased by a factor F at one location is balanced by $(F–1)$ other locations with zero percolation and zero seepage. The seep flow rate Q_s is not reduced because it is supposed to represent the average seep flow rate for locations with seepage; thus, adding any number of non-seeping locations does not change it. The total effect is to reduce the seepage fraction and increase the seep flow rate from the results that do not account for flow focusing.

6.3.4 Episodic Flow

As discussed in Section 5, we assume for the seepage abstraction analysis/model that episodic flow can be neglected, because there is no evidence for it at the repository depth and flow simulations have shown that the Paintbrush nonwelded unit above the repository damps out episodic flow. However, it would be relatively easy to approximate episodic effects in the seepage abstraction, and for completeness this subsection explains how it could be done.

Episodic flow can increase the amount of seepage for a given yearly flux because, if flow only occurs a portion of the year, the percolation flux must be higher during the periods when flow does occur. This effect was confirmed by three seepage simulations for an example episodic-flow scenario (CRWMS M&O 2000a, Section 6.6.7). As would be expected, the seepage rate cycles up and down with the percolation flux, and the peak value of the seepage percentage is approximately what would be expected based on the peak value of the percolation flux (CRWMS M&O 2000a, Section 6.6.7). It is also noted there that the average seepage percentage (averaged over both wet and dry periods) is significantly lower than the peak values.

As with flow focusing, there is a simple approximation for this effect. If the initial estimate of percolation flux at a location is q_i and the fraction of the time that flow occurs is E, then during flowing periods the percolation flux is given by $q = q_i/E$. The seepage fraction f_s and seep flow rate Q_s for the wet period are calculated (or sampled from distributions) based on that flux. Further modification is necessary in order to preserve the correct time-average flux. If the seep

flow rate is Q_s during the wet period and approximately zero during the dry period, the average seep flow rate over both periods is EQ_s. The effective seepage fraction should remain at f_s because that is the fraction of locations that have seepage, but the seepage occurs for only a fraction of the time rather than being continuous.

6.3.5 Coupled Processes

Coupled processes include the various thermally driven processes that could affect seepage into emplacement drifts, including thermal-hydrologic, thermal-hydrologic-mechanical, and thermal-hydrologic-chemical processes. As discussed in Section 5, thermal-hydrologic-chemical processes have been found to have little effect on seepage. Thermal-hydrologic-mechanical processes are neglected because process-model results are not available at this time. Unlike effects of episodic flow, there is no simple abstraction for the possible effects of these processes, so they will not be discussed further.

Thermal-hydrologic effects on seepage, not counting the permanent changes in hydrologic properties that could possibly be caused by mechanical or chemical processes, are transient and consist of potential effects such as reduced seepage for a time because of thermal dryout or increased seepage during the heat-up and cool-down phases because of drainage of thermally mobilized water. An approximate method for including thermal effects on seepage is to use percolation flux above the emplacement drifts from a thermal-hydrology model as input to the seepage abstraction, rather than percolation flux from the isothermal UZ flow model. That way, if the thermal-hydrology model indicates a period of increased liquid flow because of condensate drainage, it will automatically be translated to an increase in seepage during that period. However, in order to be conservative, if the thermal-hydrology model indicates a period of reduced liquid flow because of dryout of the rock around a drift, seepage should instead be continued at its ambient (pre-heating) level through that period, in recognition that it may be possible for rapid fracture flow in discrete flow paths to penetrate the hot rock and reach the drift. Only the fracture component of the liquid flux should be taken from the thermal-hydrology model, because capillarity in the rock matrix is high enough that matrix flow would not seep into the drifts.

6.4 SUMMARY OF ABSTRACTION OF SEEPAGE INTO DRIFTS

The abstraction of drift seepage, as described in the preceding sections, consists of three parts:

1) Distributions for the amount of seepage as a function of percolation flux, derived directly from seepage process-model results (CRWMS M&O 2000a) and constrained by measurements of permeability around three niches in the ESF (CRWMS M&O 2000c, Section 6.1) and calibration of seepage tests conducted in one niche in the ESF (CRWMS M&O 2000d, Section 6.4)—see Table 8

2) Increase of the seep flow rates from (1) by 55% to adjust for effects of drift degradation and rock bolts and by 10% to account for the possibility that the fracture k and α parameters may be correlated—see Sections 6.3.1 and 6.3.2

3) Distributions of the degree of flow focusing above the drifts, based on estimates of "weep" spacings implied by the active-fracture model of UZ flow. The flow-focusing factor is used to scale the percolation flux and the seepage fraction; it is log-uniformly distributed, with minimum of 1 and maximums of 47 for the low-infiltration case, 22 for the base-infiltration case, and 9.7 for the high-infiltration case—see Section 6.3.3.2

As discussed in Section 6.2.3, seepage is a function of the ratio of geometric-mean fracture permeability to fracture air-entry parameter, $\bar{k}/\alpha$, and the uncertainty in this ratio is taken to be one order of magnitude above and one-half order of magnitude below the best-estimate value, which is 6×10^{-11} m^2·Pa. A triangular shape is chosen for the seepage uncertainty distributions. This distribution appropriately represents the key features desired, which are that seepage values for $\bar{k}/\alpha = 6 \times 10^{-11}$ m^2·Pa are most likely and that $\bar{k}/\alpha$ could be an order of magnitude higher or one-half order of magnitude lower, but those values are less likely to be representative of repository conditions.

Table 11 summarizes the seepage distributions as they vary with percolation flux. The table was generated from Table 8 by multiplying all the seep flow rates (mean and standard deviation) by 1.7 (1.55 × 1.1), and using the $\bar{k}/\alpha = 6 \times 10^{-10}$ columns for the minimum of the seepage distributions, the $\bar{k}/\alpha = 6 \times 10^{-11}$ columns for the peak of the triangular seepage distributions, and the $\bar{k}/\alpha = 2 \times 10^{-11}$ columns for the maximum of the seepage distributions. For values of percolation flux not in the table, linear interpolation or extrapolation should be used. The values in Table 11 are shown graphically in Figure 2, Figure 3, and Figure 4 (note that a few additional points are plotted in the figures, obtained by linear interpolation and extrapolation).

Table 11. Uncertainty in Seepage Parameters as Function of Percolation

	Minimum Value			Peak Value			Maximum Value		
q (mm/yr)	f_s	Mean Q_s (m^3/yr)	Std.Dev. Q_s (m^3/yr)	f_s	Mean Q_s (m^3/yr)	Std.Dev. Q_s (m^3/yr)	f_s	Mean Q_s (m^3/yr)	Std.Dev. Q_s (m^3/yr)
5	0	0	0	0	0	0	1.97×10^{-3}	3.21×10^{-3}	3.16×10^{-3}
14.6	0	0	0	2.45×10^{-3}	7.95×10^{-3}	7.09×10^{-3}	5.75×10^{-2}	2.26×10^{-2}	2.45×10^{-2}
73.2	0	0	0	0.250	0.106	0.198	0.744	0.404	0.409
213	4.91×10^{-3}	0.284	0.188	0.487	1.51	1.15	0.944	3.31	2.24
500	6.01×10^{-2}	0.992	1.05	0.925	5.50	4.48	0.999	13.0	5.74

Taken from Excel spreadsheet Seep-sr.xls, submitted with this report under DTN: SN9912T0511599.002.

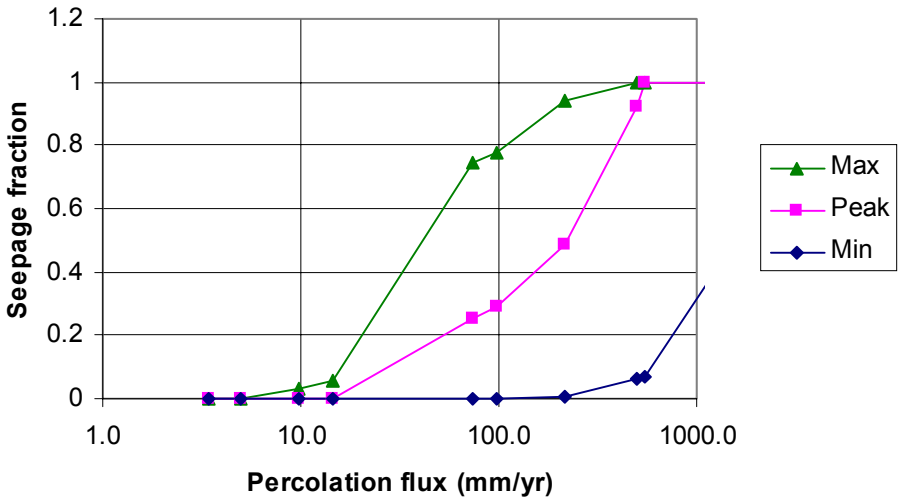

Figure 2. Seepage Fraction vs. Percolation Flux

Taken from Excel spreadsheet Seep-sr.xls, submitted with this report under DTN: SN9912T0511599.002.

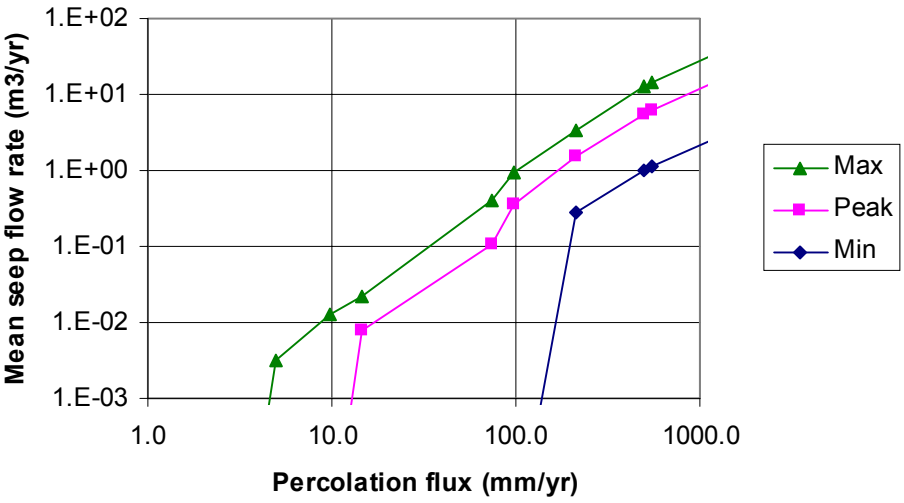

Figure 3. Mean Seep Flow Rate vs. Percolation Flux

Taken from Excel spreadsheet Seep-sr.xls, submitted with this report under DTN: SN9912T0511599.002.

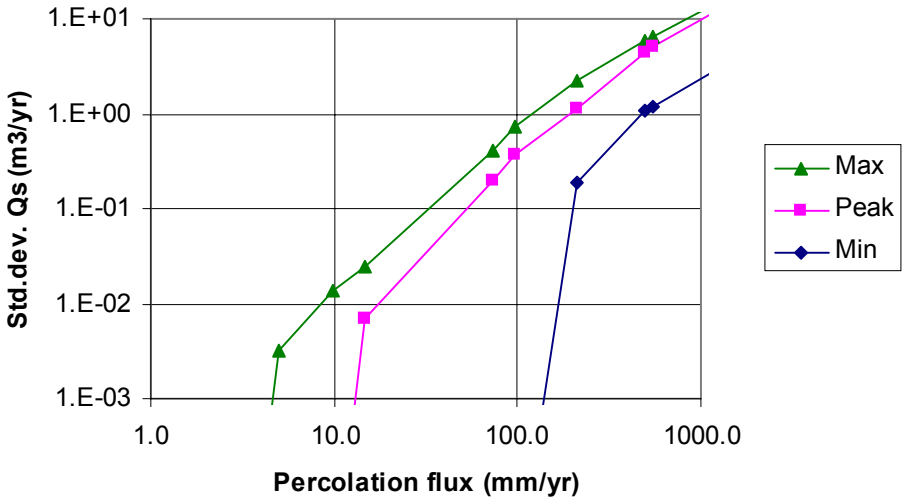

Figure 4. Std. Dev. of Seep Flow Rate vs. Percolation Flux

Taken from Excel spreadsheet Seep-sr.xls, submitted with this report under DTN: SN9912T0511599.002.

The effect of flow focusing is illustrated in Figure 5 and Figure 6, for seepage fraction and mean seep flow rate, respectively. Each plot has four curves, for the focusing factor F equal to 1 (no flow focusing), 5, 15, and 45. The F = 1 curves are based on the mean of the respective uncertainty distributions (for a triangular distribution, the mean is [min + peak + max]/3, with min, peak, and max as listed in Table 11 and plotted in Figure 2 and Figure 3). The curves with higher values of F are generated from the F = 1 curves as described in Section 6.3.3.2. The result is as expected: more focusing of flow results in lower seepage fractions and higher seep flow rates. Note, however, that at very low percolation fluxes the seepage fraction is higher for higher focusing factors, because a percolation flux below the threshold for seepage can be boosted above the threshold by the focusing multiplier.

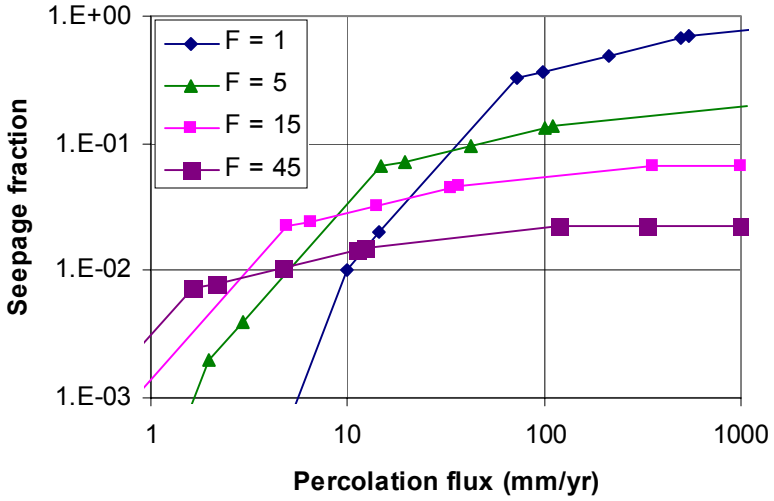

Figure 5. Effect of Flow Focusing on Seepage Fraction

Taken from Excel spreadsheet Seep-sr.xls, submitted with this report under DTN: SN9912T0511599.002.

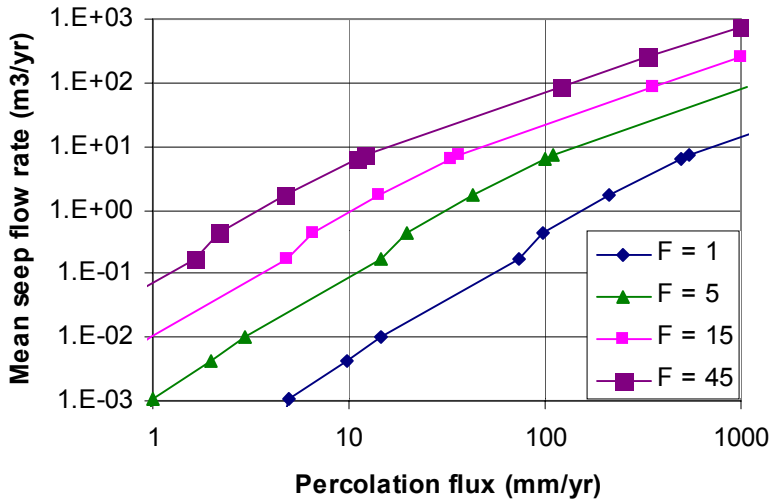

Figure 6. Effect of Flow Focusing on Mean Seep Flow Rate

Taken from Excel spreadsheet Seep-sr.xls, submitted with this report under DTN: SN9912T0511599.002.

6.5 VALIDITY OF ABSTRACTION OF SEEPAGE INTO DRIFTS

AP-3.10Q, *Analyses and Models*, requires a discussion of validation for models, with model validation defined as the process of establishing confidence that the model adequately represents the phenomena in question. The procedure points out that what is adequate depends on the intended use of the model. The purpose of the seepage abstraction is to provide estimates of the

amount of seepage into emplacement drifts for use in TSPA simulations. As such, the estimates are not expected to be accurate predictions of the future (which would be impossible), but rather they are expected to reasonably represent the range of possibilities, consistent with our uncertainties regarding the relevant processes. As has been discussed, there is considerable uncertainty about the spatial locations and quantity of seepage that will enter the emplacement drifts, but this uncertainty has been represented by means of probability distributions and conservative approximations.

Because of its probabilistic and conservative nature, it would not be appropriate to "validate" the seepage abstraction by comparing it to seepage experiments or observations and expecting a precise match. In fact, any such comparison can only be made probabilistically because all dependencies except for that on percolation flux have been removed: For a given percolation flux, the seepage abstraction gives probability distributions for the likelihood of seepage and the amount of seepage. The probability distributions include within them the likelihood of encountering various combinations of hydrologic properties within the repository and they have also been shifted to higher seepage values to account for other possible effects, such as future degradation of the drifts by rockfall. Thus, if the seepage abstraction is compared to seepage experiments or observations the expectation should be that the measured values be within the range predicted by the seepage abstraction—*or lower*. The last point is key: Because of its intended use (for TSPA simulations), it is acceptable for the seepage estimates to be high, since higher seepage would correspond to higher calculated doses in a TSPA. Of course, it is not desirable for the seepage estimates to be *too* high, and some of the conservatism could potentially be removed by collecting more seepage data in order to reduce the uncertainties.

With this understanding of the appropriate expectations for the seepage-abstraction model, its "validity" can now be discussed. The seepage probability distributions that constitute the seepage abstraction are based directly on the results of the Seepage Model for PA, so the validity of the seepage abstraction derives from the validity of that model, which in turn comes from the use of accepted approaches and site-specific seepage data (CRWMS M&O 2000a, Section 6.2). The parameters used in developing the abstraction (e.g., fracture permeability and α parameter) are reasonable and consistent with available data. Where such data are not available, as for the Topopah Spring lower lithophysal and lower nonlithophysal units, estimates of the resulting uncertainty have been included.

It is of some interest to compare the seep flow rates for the seepage abstraction to those obtained with the Seepage Calibration Model (CRWMS M&O 2000d, Figure 27). The seepage threshold (that is, the percolation flux below which there is no seepage) for the 3-D heterogeneous seepage calibration model is approximately 250 mm/yr (CRWMS M&O 2000d, Section 6.6). The seepage percentage for a percolation flux of 500 mm/yr is approximately 24% (CRWMS M&O 2000d, Figure 27). Converting that seepage percentage to a seep flow rate as described in Section 6.2.1 results in a flow rate of about 3.5 m^3/yr. Note that the seepage-calibration results for these percolation values represent an extrapolation downward from the very high fluxes used in the seepage tests and so are not directly supported by data. Note also that the geometry of the niche modeled by the Seepage Calibration Model is somewhat different from the geometry of the emplacement drifts (see Section 6.2.2), but they are similar enough that the results should be comparable. The range of seepage thresholds for the seepage abstraction (Figure 3) is well below the seepage-calibration value of 250 mm/yr. Since a lower seepage threshold implies

more seepage at low percolation fluxes, this result means that the seepage-abstraction estimate is high for low percolations, which is appropriate and expected, as discussed above. The seep flow rate of 3.5 m^3/yr at percolation flux of 500 mm/yr is within the range for the seepage abstraction (Table 11 and Figure 3): somewhat lower than the "peak," or most likely, estimate of 5.5 m^3/yr. This result is once again appropriate, given the intended use of the seepage abstraction model. These comparisons provide some additional confidence in the abstraction of drift seepage.

7. CONCLUSIONS

For this analysis/model, results of seepage process-model simulations for a large number of cases were synthesized, and distributions representing the uncertainty and spatial variability of seepage into drifts as a function of percolation flux were derived. The final abstraction, summarized in Section 6.4, accounts for several potentially important perturbing effects, including changes in drift shape caused by rockfall, preferential pathways resulting from degraded rock bolts, and focusing of flow above drifts. For TSPA calculations, it is recommended that fracture flux above the drifts from a thermal-hydrology model be used as the flux to feed into the seepage abstraction, in order to account for thermal effects on seepage as discussed in Section 6.3.5. There are no known restrictions for subsequent use. The qualification status of many of the data inputs needs to be verified, but no significant impact from them is expected because significant changes to the inputs are not expected. A potentially important uncertainty is whether thermal-mechanical processes might affect seepage significantly. It was assumed for this analysis/model that thermal-mechanical effects can be neglected (see assumption 4, Section 5). This assumption needs to be confirmed and has been assigned TBV #3964. The impact of this assumption is unknown, but if it is determined that thermal-mechanical effects on seepage cannot be neglected then they should be included in the seepage abstraction in a future revision.

All files associated with this analysis/model have been submitted to the TDMS under DTN: SN9912T0511599.002 and are considered unqualified pending qualification of upstream source data and confirmation of the assumption that thermal-mechanical effects can be neglected.

This document may be affected by technical product input information that requires confirmation. Any changes to the document that may occur as a result of completing the confirmation activities will be reflected in subsequent revisions. The status of the input information quality may be confirmed by review of the Document Input Reference System database.

8. REFERENCES

8.1 DOCUMENTS CITED

Bodvarsson, G.S.; Bandurraga, T.M.; and Wu, Y.S., eds. 1997. *The Site-Scale Unsaturated Zone Model of Yucca Mountain, Nevada, for the Viability Assessment*. LBNL-40376. Berkeley, California: Lawrence Berkeley National Laboratory. ACC: MOL.19971014.0232.

CRWMS M&O (Civilian Radioactive Waste Management System Management & Operating Contractor) 1998. "Unsaturated Zone Hydrology Model." Chapter 2 of *Total System*

Performance Assessment–Viability Assessment (TSPA-VA) Analyses Technical Basis Document. B00000000-01717-4301-00002 Rev. 01. Las Vegas, Nevada: CRWMS M&O. ACC: MOL.19981008.0002.

CRWMS M&O 1999a. *Work Direction and Planning Document, Seepage Models for PA and Abstraction of Drift Seepage & Drift-Scale Coupled Processes (Rev. 02), ID: U4000, U6020; Activity: SPP5210, SPP5290*. Abstract Seepage FY99 (13012220M7). Las Vegas, Nevada: CRWMS M&O. ACC: MOL.19990707.0121.

CRWMS M&O 1999b. *Analysis and Modeling Report (AMR) Development Plan (DP): U0075 Seepage Models for PA Including Drift Collapse, Rev 00*. TDP-NBS-HS-000009. Las Vegas, Nevada: CRWMS M&O. ACC: MOL.19990830.0384.

CRWMS M&O 1999c. *Conduct of Performance Assessment*. Activity Evaluation, September 30, 1999. Las Vegas, Nevada: CRWMS M&O. ACC: MOL.19991028.0092.

CRWMS M&O 1999d. *Development Plan: Features, Events, and Processes in UZ Flow and Transport, Rev. 00*. TDP-NBS-MD-000001. Las Vegas, Nevada: CRWMS M&O. ACC: MOL.19990719.0073.

CRWMS M&O 1999e. *Development Plan: Features, Events, and Processes in Thermal Hydrology and Coupled Processes, Rev. 00*. TDP-NBS-MD-000004. Las Vegas, Nevada: CRWMS M&O. ACC: MOL.19990819.0004.

CRWMS M&O 1999f. *Drift Degradation Analysis*. ANL-EBS-MD-000027, Rev. 00. Las Vegas, Nevada: CRWMS M&O. ACC: MOL.20000107.0328.

CRWMS M&O 1999g. *Request for Repository Subsurface Design Information to Support TSPA-SR*. Input transmittal PA-SSR-99218.Ta. Las Vegas, Nevada: CRWMS M&O. ACC: MOL.19990901.0312.

CRWMS M&O 2000a. *Seepage Model for PA Including Drift Collapse*. MDL-NBS-HS-000002, Rev. 00. Las Vegas, Nevada: CRWMS M&O. ACC: MOL.19990721.0526.

CRWMS M&O 2000b. *Drift-Scale Coupled Processes (Drift-Scale Test and THC Seepage) Models*. MDL-NBS-HS-000001, Rev. 00. Las Vegas, Nevada: CRWMS M&O. ACC: MOL.19990721.0523.

CRWMS M&O 2000c. *In Situ Field Testing of Processes*. ANL-NBS-HS-000005, Rev. 00. Las Vegas, Nevada: CRWMS M&O. ACC: MOL.19990721.0522.

CRWMS M&O 2000d. *Seepage Calibration Model and Seepage Testing Data*. MDL-NBS-HS-000004, Rev. 00. Las Vegas, Nevada: CRWMS M&O. ACC: MOL.19990721.0521.

CRWMS M&O 2000e. *Calibrated Properties Model*. MDL-NBS-HS-000003, Rev. 00. Las Vegas, Nevada: CRWMS M&O. ACC: MOL.19990721.0520.

DOE (U.S. Department of Energy) 1998. *Total System Performance Assessment.* Volume 3 of *Viability Assessment of a Repository at Yucca Mountain*. DOE/RW-0508/V3. Washington, D.C.: U.S. Department of Energy, Office of Civilian Radioactive Waste Management. ACC: MOL.19981007.0030.

DOE 2000. *Quality Assurance Requirements and Description*. DOE/RW-0333P, Rev. 9. Washington, D.C.: U.S. Department of Energy, Office of Civilian Radioactive Waste Management. ACC: MOL.19991028.0012.

Dyer, J.R. 1999. "Revised Interim Guidance Pending Issuance of New U.S. Nuclear Regulatory Commission (NRC) Regulations (Revision 01, July 22, 1999), for Yucca Mountain, Nevada." Letter from J.R. Dyer (DOE) to Dr. D.R. Wilkins (CRWMS M&O), September 3, 1999, OL&RC:SB-1714, with enclosure, "Interim Guidance Pending Issuance of New NRC Regulations for Yucca Mountain (Revision 01)." ACC: MOL.19990910.0079.

Glass, R.J. and Tidwell, V.C. 1991. *Research Program to Develop and Validate Conceptual Models for Flow and Transport Through Unsaturated, Fractured Rock*. SAND90-2261. Albuquerque, New Mexico: Sandia National Laboratories. ACC: NNA.19910906.0001.

Ho, C.K. and Wilson, M.L. 1998. "Calculation of Discrete Fracture Flow Paths in Dual-Continuum Models." *High-Level Radioactive Waste Management, Proceedings of the Eighth International Conference, Las Vegas, Nevada, May 11–14, 1998*, 375–377. La Grange Park, Illinois: American Nuclear Society. TIC: 237082.

Liu, H.H.; Doughty, C.; and Bodvarsson, G.S. 1998. "An Active Fracture Model for Unsaturated Flow and Transport in Fractured Rocks." *Water Resources Research*, *34* (10), 2633–2646. Washington, D.C.: American Geophysical Union. TIC: 243012.

8.2 PROCEDURES CITED

AP-3.10Q, Rev. 2, ICN 0. *Analyses and Models*. Washington, D.C.: U.S. Department of Energy, Office of Civilian Radioactive Waste Management. ACC: MOL.20000217.0246.

AP-3.14Q, Rev. 0, ICN 0. *Transmittal of Input*. Washington, D.C.: U.S. Department of Energy, Office of Civilian Radioactive Waste Management. ACC: MOL.19990701.0621.

AP-3.15Q, Rev. 1, ICN 1. *Managing Technical Product Inputs*. Washington, D.C.: U.S. Department of Energy, Office of Civilian Radioactive Waste Management. ACC: MOL.20000218.0069.

AP-SI.1Q, Rev. 2, ICN 4. *Software Management*. Washington, D.C.: U.S. Department of Energy, Office of Civilian Radioactive Waste Management. ACC: MOL.20000223.0508.

QAP-2-0, Rev. 5, ICN 0. *Conduct of Activities*. Las Vegas, Nevada: CRWMS M&O. ACC: MOL.19980826.0209.

8.3 SOURCE DATA, LISTED BY DATA TRACKING NUMBER

LB990501233129.001. Fracture Properties for the UZ Model Grids and Uncalibrated Fracture and Matrix Properties for the UZ Model Layers for AMR U0090, "Analysis of Hydrologic Properties Data." Submittal date: 08/25/1999.

LB990701233129.001. 3-D UZ Model Grids for Calculation of Flow Fields for PA for AMR U0000, "Development of Numerical Grids for UZ Flow and Transport Modeling." Submittal date: 09/24/1999.

LB990801233129.007. TSPA Grid Flow Simulations for AMR U0050, "UZ Flow Models and Submodels." (Flow Field #7). Submittal date: 11/29/1999.

LB990801233129.009. TSPA Grid Flow Simulations for AMR U0050, "UZ Flow Models and Submodels." (Flow Field #9). Submittal date: 11/29/1999.

LB990801233129.011. TSPA Grid Flow Simulations for AMR U0050, "UZ Flow Models and Submodels." (Flow Field #11). Submittal date: 11/29/1999.

LB990831012027.001. Input to Seepage Calibration Model AMR U0080. Submittal date: 08/31/1999.

LB990861233129.001. Drift Scale Calibrated 1-D Property Set, FY99. Submittal date: 08/06/1999.

LB990861233129.002. Drift Scale Calibrated 1-D Property Set, FY99. Submittal date: 08/06/1999.

LB990861233129.003. Drift Scale Calibrated 1-D Property Set, FY99. Submittal date: 08/06/1999.

LB990901233124.004. Air Permeability Cross-Hole Connectivity in Alcove 6, Alcove 4, and Niche 4 of the ESF for AMR U0015, "In Situ Testing of Field Processes." Submittal date: 11/01/1999.

LB991101233129.002. Percent Seepage Predictions from Seepage Model for PA in AMR U0075, "Seepage Model for PA Including Drift Collapse." Submittal date: 11/30/1999.

LB997141233129.001. Calibrated Base-case Infiltration 1-D Parameter Set for the UZ Flow and Transport Model, FY99. Submittal date: 07/21/1999.

LB997141233129.002. Calibrated Upper-Bound Infiltration 1-D Parameter Set For the UZ Flow and Transport Model, FY99. Submittal date: 07/21/1999.

LB997141233129.003. Calibrated Lower-Bound Infiltration 1-D Parameter Set for the UZ Flow and Transport Model, FY99. Submittal date: 07/21/1999.

SN9907T0872799.001. Heat Decay Data and Repository Footprint for Thermal-Hydrologic and Conduction-Only Models for TSPA-SR. Submittal date: 07/27/1999.

SN9908T0872799.004. Tabulated In-Drift Geometric and Thermal Properties Used in Drift-Scale Models for TSPA-SR. Submittal date: 08/30/1999.

9. ATTACHMENTS

Attachment	Title
I	Software Routine T2WEEP v. 1.0
II	Repository Elements
III	Directory of files submitted to TDMS (DTN: SN9912T0511599.002)

ATTACHMENT I

Software Routine T2WEEP v. 1.0

This attachment contains sample input/output files and the source listing for T2WEEP v. 1.0. A description of the use and verification of this software routine is presented in Section 6.3.3.1. Spot checks were performed on the output files to ensure that the routine was performing correctly for the range of input parameters used. An example of a spot check is provided as follows, for the reported percolation flux and weep spacings for the first repository element, 'fph 2.' (Note: although the repository percolation flux is not used in this AMR, its value may be used in future analyses). To calculate the repository percolation flux in mm/year, we need the mass flow rate between this element and the element above it (kg/s), the connection area between the two elements (m^2), and the liquid density (kg/m^3).

The mass flow rate between 'fph 2' and the element above it 'foh 2' is given in 'pa_glam1.out' in DTN: LB990801233129.009 as 0.10675E–01 kg/s. The connection area between element 'fph 2' and the element above it is reported in the mesh file (DTN: LB990701233129.001) as 0.4311E+05 m^2. The water liquid density is equal to 1000 kg/m^3 (consistent with the value assumed in the UZ site-scale model to calculate infiltration). The percolation flux can then be calculated as follows: percolation flux = (0.10675E–01 kg/s) ÷ (0.4311E+05 m^2) ÷ (1000 kg/m^3) = 2.476E–10 m/s. This value can be converted to mm/yr as follows: (2.476E–10 m/s) × (1000 mm/m) × (3.1536E+07 s/yr) = 7.809 mm/yr. This is exactly the number that is reported in the sample output file (see below).

The two weep spacings for element 'fph 2' are calculated using the formulation provided in Eqs. 6–8 of this report. The first weep spacing is calculated using the A^* parameter (DTN: LB990501233129.001) and the residual fracture saturation (DTN: LB997141233129.001, DTN: LB997141233129.002, and DTN: LB997141233129.003), as well as the fracture saturation provided in 'pa_glam1.out' (DTN: LB990801233129.009). The A^* parameter is equal to 12.31 (1/m), and the residual fracture liquid saturation is equal to 0.01. The fracture liquid saturation is equal to 0.15007E–01. Substituting these values into Eqs. 6 and 7 yields the first weep spacing as 32.12 m, which is exactly the value reported in the sample output file below.

The second weep spacing is given by Eq. 8. For this calculation, the geometric fracture spacing (DTN: LB990501233129.001) and the γ parameter are required (DTN: LB997141233129.001, DTN: LB997141233129.002, and DTN: LB997141233129.003). The geometric fracture spacing and the γ parameter for this test case are equal to 0.25 m and 0.41, respectively. Substituting the required values into Eq. 8 yields a second weep spacing of 2.184 m, which is exactly the value reported in the sample output file below.

I.1 Sample Input File

```
/home/ckho/tspaSR-LA/base-case_flow_fields/LBNL_grid/SR-repo-nodes
../pa_glam1.out
/home/ckho/tspaSR-LA/base-case_flow_fields/LBNL_grid/lb990701233129.001/mpa_pch1.v1
glam1_weep.out
0.01
1000.
.41,.41,.41,.5
13.54,9.68,12.31,8.6
0.23,0.32,0.25,0.59

#The gamma values are taken from DTN: LB997141233129.001.  The values are
#different for lower, mean, and upper infiltration models, but they are
#the same for perched water models #1 and #2 and for future climates.
#The (Afm/V) parameter and fracture spacings(1/frequency) are taken from
#DTN: LB990501233129.001 (AMR U0090), and they are constant.
--------------------------
      write(*,*)'What is the name of repository element file?'
      read(*,*) repo
      write(*,*) 'What is the name of the TOUGH2 output file?'
      read(*,*) t2out
      write(*,*) 'What is the name of the TOUGH2 mesh file?'
      read(*,*) t2mesh
      write(*,*) 'What would you like to name your output file?'
      read(*,*) output
      write(*,*)'What is the residual fracture liquid saturation?'
      read(*,*) sfr
      write(*,*)'What is the liquid density (kg/m^3)?'
      read(*,*) rho
      write(*,*)'What are the gamma parameters for the units:'
      write(*,*)'tswF4, tswF5, tswF6, and tswFf?'
      read(*,*) g4,g5,g6,gf
      write(*,*)'What are the (Afm/V) parameters for the units:'
      write(*,*)'tswF4, tswF5, tswF6, and tswFf?'
      read(*,*) afm4,afm5,afm6,afmf
      write(*,*)'Geometric fracture spacings (m) for the units:'
      write(*,*)'tswF4, tswF5, tswF6, and tswFf?'
      read(*,*) d4,d5,d6,df
```

I.2 Sample Output file

Screen Output File:

```
What is the name of repository element file?
 What is the name of the TOUGH2 output file?
 What is the name of the TOUGH2 mesh file?
 What would you like to name your output file?
 What is the residual fracture liquid saturation?
 What is the liquid density (kg/m^3)?
 What are the gamma parameters for the units:
 tswF4, tswF5, tswF6, and tswFf?
 What are the (Afm/V) parameters for the units:
 tswF4, tswF5, tswF6, and tswFf?
 Geometric fracture spacings (m) for the units:
 tswF4, tswF5, tswF6, and tswFf?
Have read in  97976 elements in ELEME and
   275 repository elements in ELEME...
Have read in 396770 number of connections
and    275 number of repository connections...
Have read in    275 repository liquid saturations...
Have read in    275 repository fluxes...
```

Data Output File:

```
*** Output file from t2weep_v1.f ***
TOUGH2 output file: ../pa_glam1.out
TOUGH2 mesh file: /home/ckho/tspaSR-LA/base-case_flow_fields/LBNL_grid/lb990701233129.001/mpa_pch1.v1
Repository element file: /home/ckho/tspaSR-LA/base-case_flow_fields/LBNL_grid/SR-repo-nodes
Gamma value for tswF4, tswF5, tswF6, and tswFf:    0.41   0.41   0.41   0.50
Afm/V value for tswF4, tswF5, tswF6, and tswFf:   13.54   9.68  12.31   8.60
Fracture spacing for tswF4, tswF5, tswF6, and tswFf:    0.23   0.32   0.25   0.59
The percolation flux is that entering the listed repository
element from the element above. The first weep spacing
assumes that the fractures with weeps are saturated
(i.e., weep width in each fracture equals weep spacing).
The second weep spacing assumes that the active fractures
are unsaturated and is taken from eq. 17 of Liu et al.
(1998) WRR, 34(10), 2633-2646.
***Note that fault materials (ending in "f") are placed at the end of the file***

Element, material, x(m), y(m), z(m), Sl, percolation(mm/year), weep_spacing1(m), weep_spacing2(m)
Fph 2, tswF6,  170424.312,  231092.641,    1109.641,  0.1501E-01,  0.7809E+01,  0.3212E+02,  0.2184E+01
Foh 3, tswF5,  170681.094,  231009.219,    1109.641,  0.1484E-01,  0.4714E+01,  0.4227E+02,  0.2835E+01
Fph 4, tswF6,  170449.344,  231169.672,    1108.478,  0.1333E-01,  0.2641E+01,  0.4823E+02,  0.2580E+01
Foh 5, tswF6,  170474.375,  231246.719,    1107.315,  0.1553E-01,  0.1011E+02,  0.2911E+02,  0.2098E+01
Fph 6, tswF6,  170499.391,  231323.750,    1106.152,  0.1548E-01,  0.9875E+01,  0.2937E+02,  0.2106E+01
Fsh 7, tswF6,  170267.641,  231484.219,    1104.990,  0.1678E-01,  0.1751E+02,  0.2372E+02,  0.1929E+01
Fph 8, tswF6,  170524.422,  231400.781,    1104.990,  0.1592E-01,  0.1207E+02,  0.2719E+02,  0.2040E+01
Fph 9, tswF5,  171038.000,  231233.922,    1104.990,  0.1228E-01,  0.6374E+00,  0.8991E+02,  0.3864E+01
Fsh10, tswF6,  170292.672,  231561.250,    1103.827,  0.2076E-01,  0.5894E+02,  0.1494E+02,  0.1596E+01
Fqh11, tswF5,  170549.453,  231477.828,    1103.827,  0.2066E-01,  0.3779E+02,  0.1918E+02,  0.2051E+01
Fqh12, tswF5,  170806.234,  231394.391,    1103.827,  0.1272E-01,  0.1041E+01,  0.7523E+02,  0.3591E+01
Fsh13, tswF6,  170317.703,  231638.281,    1102.664,  0.1748E-01,  0.2252E+02,  0.2149E+02,  0.1853E+01
Fph14, tswF5,  170574.484,  231554.859,    1102.664,  0.1645E-01,  0.1014E+02,  0.3170E+02,  0.2520E+01
Fqh15, tswF5,  170831.266,  231471.422,    1102.664,  0.1276E-01,  0.1074E+01,  0.7419E+02,  0.3571E+01
Foh16, tswF5,  171088.062,  231388.000,    1102.664,  0.1440E-01,  0.3634E+01,  0.4651E+02,  0.2949E+01
Frh17, tswF6,  170342.734,  231715.328,    1101.501,  0.1440E-01,  0.5546E+01,  0.3660E+02,  0.2304E+01
Fph18, tswF5,  170599.516,  231631.891,    1101.501,  0.1865E-01,  0.2164E+02,  0.2365E+02,  0.2235E+01
Fph19, tswF5,  170856.297,  231548.469,    1101.501,  0.1454E-01,  0.3950E+01,  0.4504E+02,  0.2910E+01
Foh20, tswF5,  171113.094,  231465.031,    1101.501,  0.1437E-01,  0.3565E+01,  0.4685E+02,  0.2958E+01
Frh21, tswF6,  170367.750,  231792.359,    1100.338,  0.1715E-01,  0.1994E+02,  0.2251E+02,  0.1888E+01
Fph22, tswF5,  170624.547,  231708.938,    1100.338,  0.1628E-01,  0.9314E+01,  0.3255E+02,  0.2547E+01
Fph23, tswF5,  170881.328,  231625.500,    1100.338,  0.1308E-01,  0.1416E+01,  0.6648E+02,  0.3414E+01
Fsh24, tswF6,  170392.781,  231869.391,    1099.175,  0.1497E-01,  0.7639E+01,  0.3235E+02,  0.2191E+01
Fph25, tswF5,  170649.578,  231785.969,    1099.175,  0.1924E-01,  0.2595E+02,  0.2213E+02,  0.2175E+01
Foh26, tswF5,  170906.359,  231702.531,    1099.175,  0.1468E-01,  0.4310E+01,  0.4370E+02,  0.2874E+01
Frh27, tswF5,  170417.812,  231946.438,    1098.013,  0.1869E-01,  0.2192E+02,  0.2355E+02,  0.2231E+01
Fph28, tswF5,  170674.609,  231863.000,    1098.013,  0.1793E-01,  0.1732E+02,  0.2580E+02,  0.2316E+01
Foh29, tswF5,  170931.391,  231779.578,    1098.013,  0.1281E-01,  0.1108E+01,  0.7284E+02,  0.3544E+01
```

```
Fth30, tswF6,  170186.062,  232106.906,    1096.850,  0.1879E-01,  0.3462E+02,  0.1830E+02,  0.1734E+01
Fsh31, tswF5,  170442.844,  232023.469,    1096.850,  0.1587E-01,  0.7710E+01,  0.3483E+02,  0.2619E+01
Fph32, tswF5,  170699.625,  231940.031,    1096.850,  0.1504E-01,  0.5301E+01,  0.4060E+02,  0.2789E+01
Foh33, tswF5,  170956.422,  231856.609,    1096.850,  0.1579E-01,  0.7537E+01,  0.3533E+02,  0.2634E+01
Fuh34, tswF6,  170211.094,  232183.938,    1095.687,  0.1555E-01,  0.1022E+02,  0.2896E+02,  0.2093E+01
Fqh35, tswF5,  170467.875,  232100.500,    1095.687,  0.1882E-01,  0.2290E+02,  0.2319E+02,  0.2217E+01
Fph36, tswF5,  170724.656,  232017.078,    1095.687,  0.1806E-01,  0.1803E+02,  0.2536E+02,  0.2300E+01
Foh37, tswF5,  170981.453,  231933.641,    1095.687,  0.1519E-01,  0.5637E+01,  0.3943E+02,  0.2756E+01
Fth38, tswF6,  170236.109,  232260.969,    1094.524,  0.2056E-01,  0.5610E+02,  0.1523E+02,  0.1608E+01
Fqh39, tswF5,  170492.906,  232177.547,    1094.524,  0.1910E-01,  0.2484E+02,  0.2248E+02,  0.2189E+01
Fph40, tswF5,  170749.688,  232094.109,    1094.524,  0.1665E-01,  0.1086E+02,  0.3074E+02,  0.2488E+01
Foh41, tswF5,  171006.469,  232010.672,    1094.524,  0.1409E-01,  0.3013E+01,  0.5000E+02,  0.3037E+01
Fth42, tswF6,  170261.141,  232338.016,    1093.361,  0.1759E-01,  0.2334E+02,  0.2119E+02,  0.1842E+01
Fqh43, tswF5,  170517.938,  232254.578,    1093.361,  0.1665E-01,  0.1084E+02,  0.3076E+02,  0.2489E+01
Fph44, tswF5,  170774.719,  232171.141,    1093.361,  0.1876E-01,  0.2248E+02,  0.2335E+02,  0.2223E+01
Foh45, tswF5,  171031.500,  232087.719,    1093.361,  0.1809E-01,  0.1828E+02,  0.2527E+02,  0.2296E+01
Fqh46, tswF5,  170542.969,  232331.609,    1092.198,  0.1953E-01,  0.2811E+02,  0.2146E+02,  0.2147E+01
Fph47, tswF5,  170799.750,  232248.188,    1092.198,  0.1674E-01,  0.1122E+02,  0.3037E+02,  0.2476E+01
Foh48, tswF5,  171056.531,  232164.750,    1092.198,  0.1601E-01,  0.8266E+01,  0.3405E+02,  0.2595E+01
Fth49, tswF5,  170311.203,  232492.078,    1091.036,  0.2168E-01,  0.4801E+02,  0.1751E+02,  0.1976E+01
Frh50, tswF5,  170567.984,  232408.656,    1091.036,  0.1708E-01,  0.1277E+02,  0.2891E+02,  0.2426E+01
Fqh51, tswF5,  170824.781,  232325.219,    1091.036,  0.1543E-01,  0.6367E+01,  0.3763E+02,  0.2704E+01
Foh52, tswF5,  171081.562,  232241.781,    1091.036,  0.1773E-01,  0.1613E+02,  0.2646E+02,  0.2340E+01
Fmh53, tswF6,  170079.453,  232652.547,    1089.873,  0.2044E-01,  0.5479E+02,  0.1540E+02,  0.1616E+01
Fth54, tswF5,  170336.234,  232569.109,    1089.873,  0.1705E-01,  0.1247E+02,  0.2901E+02,  0.2430E+01
Fqh55, tswF5,  170593.016,  232485.688,    1089.873,  0.1966E-01,  0.2907E+02,  0.2119E+02,  0.2136E+01
Fph56, tswF5,  170849.812,  232402.250,    1089.873,  0.1904E-01,  0.2442E+02,  0.2263E+02,  0.2195E+01
Foh57, tswF5,  171106.594,  232318.828,    1089.873,  0.1676E-01,  0.1130E+02,  0.3026E+02,  0.2472E+01
Frh58, tswF6,  170104.484,  232729.578,    1088.710,  0.1994E-01,  0.4761E+02,  0.1619E+02,  0.1649E+01
Fth59, tswF5,  170361.266,  232646.156,    1088.710,  0.2321E-01,  0.6641E+02,  0.1549E+02,  0.1879E+01
Fqh60, tswF5,  170618.047,  232562.719,    1088.710,  0.1955E-01,  0.2820E+02,  0.2143E+02,  0.2146E+01
Frh61, tswF5,  170874.844,  232479.297,    1088.710,  0.1602E-01,  0.8358E+01,  0.3395E+02,  0.2592E+01
Foh62, tswF5,  171131.625,  232395.859,    1088.710,  0.1425E-01,  0.3347E+01,  0.4811E+02,  0.2990E+01
Fph63, tswF6,  170129.500,  232806.625,    1087.547,  0.2298E-01,  0.9666E+02,  0.1239E+02,  0.1478E+01
Fth64, tswF5,  170386.297,  232723.188,    1087.547,  0.1921E-01,  0.2560E+02,  0.2221E+02,  0.2178E+01
Fqh65, tswF5,  170643.078,  232639.750,    1087.547,  0.1643E-01,  0.9905E+01,  0.3182E+02,  0.2524E+01
Fqh66, tswF5,  170899.859,  232556.328,    1087.547,  0.1926E-01,  0.2608E+02,  0.2208E+02,  0.2172E+01
Foh67, tswF4,  171156.656,  232472.891,    1087.547,  0.2068E-01,  0.1356E+02,  0.1369E+02,  0.1473E+01
Fmh68, tswF6,  170154.531,  232883.656,    1086.384,  0.2036E-01,  0.5327E+02,  0.1552E+02,  0.1621E+01
Fth69, tswF5,  170411.328,  232800.219,    1086.384,  0.2347E-01,  0.7003E+02,  0.1519E+02,  0.1864E+01
Frh70, tswF5,  170668.109,  232716.797,    1086.384,  0.1884E-01,  0.2300E+02,  0.2315E+02,  0.2215E+01
Fqh71, tswF5,  170924.891,  232633.359,    1086.384,  0.1668E-01,  0.1100E+02,  0.3061E+02,  0.2484E+01
Foh72, tswF4,  171181.688,  232549.938,    1086.384,  0.1796E-01,  0.6203E+01,  0.1836E+02,  0.1661E+01
Frh73, tswF5,  170179.562,  232960.688,    1085.222,  0.2334E-01,  0.6833E+02,  0.1533E+02,  0.1871E+01
Fsh74, tswF5,  170436.344,  232877.266,    1085.222,  0.2135E-01,  0.4456E+02,  0.1802E+02,  0.1999E+01
Frh75, tswF5,  170693.141,  232793.828,    1085.222,  0.1657E-01,  0.1048E+02,  0.3115E+02,  0.2502E+01
Frh76, tswF5,  170949.922,  232710.391,    1085.222,  0.1467E-01,  0.4262E+01,  0.4384E+02,  0.2878E+01
Frh77, tswF5,  170204.594,  233037.719,    1084.059,  0.1657E-01,  0.1030E+02,  0.3114E+02,  0.2501E+01
Fsh78, tswF5,  170461.375,  232954.297,    1084.059,  0.1838E-01,  0.1999E+02,  0.2440E+02,  0.2263E+01
Fqh79, tswF5,  170718.172,  232870.859,    1084.059,  0.1964E-01,  0.2898E+02,  0.2121E+02,  0.2137E+01
Fph80, tswF5,  170974.953,  232787.438,    1084.059,  0.1757E-01,  0.1531E+02,  0.2701E+02,  0.2360E+01
```

```
Fsh81, tswF5,  170229.625,  233114.766,    1082.896,  0.1765E-01,  0.1560E+02,  0.2674E+02,  0.2350E+01
Fsh82, tswF5,  170486.406,  233031.328,    1082.896,  0.2263E-01,  0.5914E+02,  0.1619E+02,  0.1913E+01
Fqh83, tswF5,  170743.203,  232947.906,    1082.896,  0.1864E-01,  0.2166E+02,  0.2367E+02,  0.2236E+01
Foh84, tswF5,  170999.984,  232864.469,    1082.896,  0.1491E-01,  0.4851E+01,  0.4169E+02,  0.2819E+01
Fsh85, tswF5,  170254.656,  233191.797,    1081.733,  0.1614E-01,  0.8736E+01,  0.3329E+02,  0.2571E+01
Fsh86, tswF5,  170511.438,  233108.359,    1081.733,  0.1771E-01,  0.1598E+02,  0.2653E+02,  0.2343E+01
Fqh87, tswF5,  170768.219,  233024.938,    1081.733,  0.1612E-01,  0.8683E+01,  0.3345E+02,  0.2576E+01
Fph88, tswF5,  171025.016,  232941.500,    1081.733,  0.1827E-01,  0.1935E+02,  0.2472E+02,  0.2276E+01
Fsh89, tswF5,  170279.688,  233268.828,    1080.570,  0.1608E-01,  0.8557E+01,  0.3366E+02,  0.2583E+01
Fsh90, tswF5,  170536.469,  233185.406,    1080.570,  0.2214E-01,  0.5331E+02,  0.1684E+02,  0.1944E+01
Fqh91, tswF5,  170793.250,  233101.969,    1080.570,  0.1969E-01,  0.2932E+02,  0.2112E+02,  0.2133E+01
Foh92, tswF5,  171050.047,  233018.547,    1080.570,  0.1675E-01,  0.1131E+02,  0.3029E+02,  0.2473E+01
Fth93, tswF5,  170304.719,  233345.875,    1079.407,  0.2009E-01,  0.3272E+02,  0.2027E+02,  0.2098E+01
Fsh94, tswF5,  170561.500,  233262.438,    1079.407,  0.2007E-01,  0.3246E+02,  0.2031E+02,  0.2099E+01
Fqh95, tswF5,  170818.281,  233179.016,    1079.407,  0.1692E-01,  0.1202E+02,  0.2958E+02,  0.2449E+01
Foh96, tswF5,  171075.062,  233095.578,    1079.407,  0.1433E-01,  0.3496E+01,  0.4727E+02,  0.2968E+01
Fth97, tswF5,  170329.734,  233422.906,    1078.245,  0.1778E-01,  0.1636E+02,  0.2630E+02,  0.2334E+01
Fsh98, tswF5,  170586.531,  233339.469,    1078.245,  0.1707E-01,  0.1272E+02,  0.2894E+02,  0.2428E+01
Fph99, tswF5,  170843.312,  233256.047,    1078.245,  0.1792E-01,  0.1729E+02,  0.2581E+02,  0.2316E+01
Foi 0, tswF4,  171100.094,  233172.609,    1078.245,  0.1864E-01,  0.7284E+01,  0.1693E+02,  0.1607E+01
Fsi 1, tswF5,  170354.766,  233499.938,    1077.082,  0.2254E-01,  0.5801E+02,  0.1631E+02,  0.1919E+01
Fsi 2, tswF5,  170611.562,  233416.516,    1077.082,  0.2148E-01,  0.4595E+02,  0.1782E+02,  0.1990E+01
Fqi 3, tswF5,  170868.344,  233333.078,    1077.082,  0.1623E-01,  0.9139E+01,  0.3285E+02,  0.2557E+01
Foi 4, tswF4,  171125.125,  233249.656,    1077.082,  0.1754E-01,  0.5103E+01,  0.1940E+02,  0.1699E+01
Fsi 5, tswF5,  170379.797,  233576.984,    1075.919,  0.2061E-01,  0.3722E+02,  0.1928E+02,  0.2055E+01
Fsi 6, tswF5,  170636.578,  233493.547,    1075.919,  0.1690E-01,  0.1191E+02,  0.2966E+02,  0.2452E+01
Fsi 7, tswF5,  170893.375,  233410.109,    1075.919,  0.1944E-01,  0.2745E+02,  0.2167E+02,  0.2156E+01
Fsi 8, tswF5,  170404.828,  233654.016,    1074.756,  0.1688E-01,  0.1182E+02,  0.2973E+02,  0.2454E+01
Fsi 9, tswF5,  170661.609,  233570.578,    1074.756,  0.1994E-01,  0.3145E+02,  0.2057E+02,  0.2110E+01
Fqi10, tswF5,  170918.406,  233487.156,    1074.756,  0.1818E-01,  0.1879E+02,  0.2502E+02,  0.2287E+01
Fri11, tswF5,  170173.062,  233814.484,    1073.593,  0.1708E-01,  0.1283E+02,  0.2890E+02,  0.2426E+01
Fsi12, tswF5,  170429.859,  233731.047,    1073.593,  0.2241E-01,  0.5642E+02,  0.1649E+02,  0.1927E+01
Fri13, tswF5,  170686.641,  233647.625,    1073.593,  0.1698E-01,  0.1232E+02,  0.2930E+02,  0.2440E+01
Fri14, tswF5,  170943.438,  233564.188,    1073.593,  0.1559E-01,  0.6935E+01,  0.3660E+02,  0.2673E+01
Fri15, tswF5,  170198.094,  233891.516,    1072.431,  0.1426E-01,  0.3343E+01,  0.4798E+02,  0.2987E+01
Fsi16, tswF5,  170454.891,  233808.078,    1072.431,  0.1671E-01,  0.1106E+02,  0.3048E+02,  0.2480E+01
Fri17, tswF5,  170711.672,  233724.656,    1072.431,  0.1976E-01,  0.2988E+02,  0.2097E+02,  0.2127E+01
Fqi18, tswF5,  170968.453,  233641.219,    1072.431,  0.2019E-01,  0.3357E+02,  0.2007E+02,  0.2089E+01
Fqi19, tswF4,  171225.250,  233557.797,    1072.431,  0.2400E-01,  0.2781E+02,  0.1045E+02,  0.1318E+01
Fsi20, tswF5,  170223.125,  233968.547,    1071.268,  0.1519E-01,  0.5649E+01,  0.3940E+02,  0.2755E+01
Fsi21, tswF5,  170479.922,  233885.125,    1071.268,  0.2158E-01,  0.4703E+02,  0.1766E+02,  0.1983E+01
Fri22, tswF5,  170736.703,  233801.688,    1071.268,  0.1999E-01,  0.3182E+02,  0.2048E+02,  0.2107E+01
Fsi23, tswF5,  170248.156,  234045.594,    1070.105,  0.1352E-01,  0.2027E+01,  0.5809E+02,  0.3230E+01
Fsi24, tswF5,  170504.938,  233962.156,    1070.105,  0.1675E-01,  0.1126E+02,  0.3029E+02,  0.2473E+01
Fsi25, tswF5,  170761.734,  233878.719,    1070.105,  0.1610E-01,  0.8657E+01,  0.3351E+02,  0.2578E+01
Fri26, tswF4,  171018.516,  233795.297,    1070.105,  0.2473E-01,  0.3052E+02,  0.9924E+01,  0.1291E+01
Fsi27, tswF5,  170273.188,  234122.625,    1068.942,  0.1238E-01,  0.6689E+00,  0.8605E+02,  0.3795E+01
Fsi28, tswF5,  170529.969,  234039.188,    1068.942,  0.2247E-01,  0.5714E+02,  0.1641E+02,  0.1923E+01
Fri29, tswF5,  170786.766,  233955.766,    1068.942,  0.1938E-01,  0.2703E+02,  0.2180E+02,  0.2161E+01
Fri30, tswF4,  171043.547,  233872.328,    1068.942,  0.2003E-01,  0.1090E+02,  0.1458E+02,  0.1512E+01
Fsi31, tswF5,  170298.219,  234199.656,    1067.779,  0.1522E-01,  0.5824E+01,  0.3922E+02,  0.2749E+01
```

```
Fsi32, tswF5,  170555.000,  234116.234,    1067.779,  0.2037E-01,  0.3511E+02,  0.1972E+02,  0.2074E+01
Fri33, tswF5,  170811.797,  234032.797,    1067.779,  0.1614E-01,  0.8783E+01,  0.3330E+02,  0.2571E+01
Fqi34, tswF4,  171068.578,  233949.359,    1067.779,  0.1637E-01,  0.3281E+01,  0.2294E+02,  0.1820E+01
Fsi35, tswF5,  170323.250,  234276.703,    1066.616,  0.1420E-01,  0.3234E+01,  0.4867E+02,  0.3004E+01
Fsi36, tswF5,  170580.031,  234193.266,    1066.616,  0.1660E-01,  0.1063E+02,  0.3097E+02,  0.2496E+01
Fqi37, tswF5,  170836.812,  234109.828,    1066.616,  0.1834E-01,  0.1980E+02,  0.2453E+02,  0.2268E+01
Fpi38, tswF4,  171093.609,  234026.406,    1066.616,  0.1821E-01,  0.6709E+01,  0.1781E+02,  0.1641E+01
Fsi39, tswF5,  170348.281,  234353.734,    1065.454,  0.2016E-01,  0.3333E+02,  0.2013E+02,  0.2092E+01
Fri40, tswF5,  170605.062,  234270.297,    1065.454,  0.2225E-01,  0.5457E+02,  0.1669E+02,  0.1937E+01
Fqi41, tswF5,  170861.844,  234186.875,    1065.454,  0.1713E-01,  0.1302E+02,  0.2870E+02,  0.2419E+01
Fpi42, tswF4,  171118.641,  234103.438,    1065.454,  0.1587E-01,  0.2781E+01,  0.2490E+02,  0.1883E+01
Fsi43, tswF5,  170373.312,  234430.766,    1064.291,  0.1915E-01,  0.2532E+02,  0.2236E+02,  0.2184E+01
Fsi44, tswF5,  170630.094,  234347.344,    1064.291,  0.1741E-01,  0.1440E+02,  0.2759E+02,  0.2380E+01
Fqi45, tswF5,  170886.875,  234263.906,    1064.291,  0.1486E-01,  0.4740E+01,  0.4206E+02,  0.2830E+01
Fpi46, tswF4,  171143.656,  234180.469,    1064.291,  0.2020E-01,  0.1202E+02,  0.1434E+02,  0.1501E+01
Fsi47, tswF5,  170398.328,  234507.797,    1063.128,  0.1701E-01,  0.1248E+02,  0.2916E+02,  0.2435E+01
Fri48, tswF5,  170655.125,  234424.375,    1063.128,  0.2111E-01,  0.4213E+02,  0.1841E+02,  0.2017E+01
Fpi49, tswF5,  170911.906,  234340.938,    1063.128,  0.1843E-01,  0.2031E+02,  0.2427E+02,  0.2258E+01
Fqi50, tswF4,  171168.688,  234257.516,    1063.128,  0.1931E-01,  0.9450E+01,  0.1570E+02,  0.1558E+01
Fsi51, tswF5,  170423.359,  234584.844,    1061.965,  0.2351E-01,  0.7074E+02,  0.1514E+02,  0.1861E+01
Fri52, tswF5,  170680.156,  234501.406,    1061.965,  0.1948E-01,  0.2767E+02,  0.2158E+02,  0.2152E+01
Fri53, tswF5,  170936.938,  234417.984,    1061.965,  0.1556E-01,  0.6754E+01,  0.3678E+02,  0.2678E+01
Fri54, tswF4,  171193.719,  234334.547,    1061.965,  0.1785E-01,  0.5997E+01,  0.1864E+02,  0.1672E+01
Fsi55, tswF5,  170448.391,  234661.875,    1060.802,  0.1732E-01,  0.1392E+02,  0.2795E+02,  0.2393E+01
Fsi56, tswF5,  170705.172,  234578.438,    1060.802,  0.1729E-01,  0.1382E+02,  0.2805E+02,  0.2397E+01
Fri57, tswF5,  170961.969,  234495.016,    1060.802,  0.1947E-01,  0.2767E+02,  0.2159E+02,  0.2153E+01
Fqi58, tswF4,  171218.750,  234411.578,    1060.802,  0.2151E-01,  0.1658E+02,  0.1271E+02,  0.1429E+01
Fsi59, tswF5,  170473.422,  234738.906,    1059.640,  0.2375E-01,  0.7442E+02,  0.1487E+02,  0.1848E+01
Fri60, tswF5,  170730.203,  234655.484,    1059.640,  0.2165E-01,  0.4770E+02,  0.1756E+02,  0.1978E+01
Fpi61, tswF5,  170987.000,  234572.047,    1059.640,  0.1751E-01,  0.1497E+02,  0.2723E+02,  0.2368E+01
Fpi62, tswF4,  171243.781,  234488.625,    1059.640,  0.1696E-01,  0.4352E+01,  0.2101E+02,  0.1756E+01
Fsi63, tswF5,  170498.453,  234815.953,    1058.477,  0.2140E-01,  0.4502E+02,  0.1795E+02,  0.1996E+01
Fri64, tswF5,  170755.234,  234732.516,    1058.477,  0.1693E-01,  0.1206E+02,  0.2951E+02,  0.2447E+01
Fpi65, tswF5,  171012.031,  234649.094,    1058.477,  0.1529E-01,  0.5940E+01,  0.3865E+02,  0.2733E+01
Fpi66, tswF4,  171268.812,  234565.656,    1058.477,  0.2042E-01,  0.1272E+02,  0.1403E+02,  0.1488E+01
Fsi67, tswF5,  170523.484,  234892.984,    1057.314,  0.1882E-01,  0.2283E+02,  0.2320E+02,  0.2217E+01
Fqi68, tswF5,  170780.266,  234809.547,    1057.314,  0.1970E-01,  0.2942E+02,  0.2109E+02,  0.2132E+01
Foi69, tswF5,  171037.047,  234726.125,    1057.314,  0.1932E-01,  0.2648E+02,  0.2195E+02,  0.2167E+01
Fqi70, tswF5,  170548.516,  234970.016,    1056.151,  0.2076E-01,  0.3874E+02,  0.1900E+02,  0.2043E+01
Fqi71, tswF5,  170805.297,  234886.594,    1056.151,  0.1895E-01,  0.2378E+02,  0.2286E+02,  0.2204E+01
Fpi72, tswF5,  171062.078,  234803.156,    1056.151,  0.1546E-01,  0.6499E+01,  0.3748E+02,  0.2699E+01
Fqi73, tswF5,  170573.531,  235047.062,    1054.988,  0.1584E-01,  0.7666E+01,  0.3500E+02,  0.2624E+01
Fpi74, tswF5,  170830.328,  234963.625,    1054.988,  0.1648E-01,  0.1017E+02,  0.3157E+02,  0.2515E+01
Foi75, tswF5,  171087.109,  234880.188,    1054.988,  0.1785E-01,  0.1678E+02,  0.2604E+02,  0.2325E+01
Fqi76, tswF5,  170598.562,  235124.094,    1053.825,  0.2144E-01,  0.4555E+02,  0.1787E+02,  0.1992E+01
Fpi77, tswF5,  170855.359,  235040.656,    1053.825,  0.1816E-01,  0.1881E+02,  0.2507E+02,  0.2289E+01
Fqi78, tswF5,  171112.141,  234957.234,    1053.825,  0.1578E-01,  0.7501E+01,  0.3541E+02,  0.2637E+01
Foi79, tswF5,  170623.594,  235201.125,    1052.663,  0.2173E-01,  0.4839E+02,  0.1744E+02,  0.1972E+01
Fqi80, tswF5,  170880.391,  235117.703,    1052.663,  0.1602E-01,  0.8309E+01,  0.3396E+02,  0.2592E+01
Fqi81, tswF5,  171137.172,  235034.266,    1052.663,  0.1680E-01,  0.1153E+02,  0.3008E+02,  0.2466E+01
Fmi82, tswF5,  170648.625,  235278.156,    1051.500,  0.1900E-01,  0.2441E+02,  0.2274E+02,  0.2199E+01
```

```
Fsi83, tswF5,  170905.406,  235194.734,    1051.500,  0.2058E-01,  0.3696E+02,  0.1934E+02,  0.2058E+01
Fsi84, tswF5,  171162.203,  235111.297,    1051.500,  0.1779E-01,  0.1648E+02,  0.2624E+02,  0.2332E+01
Fri85, tswF5,  170416.875,  235438.625,    1050.337,  0.1998E-01,  0.3177E+02,  0.2049E+02,  0.2107E+01
Fqi86, tswF5,  170673.656,  235355.203,    1050.337,  0.2026E-01,  0.3411E+02,  0.1994E+02,  0.2084E+01
Fsi87, tswF5,  170930.438,  235271.766,    1050.337,  0.1604E-01,  0.8425E+01,  0.3388E+02,  0.2589E+01
Fsi88, tswF5,  171187.234,  235188.344,    1050.337,  0.1726E-01,  0.1375E+02,  0.2816E+02,  0.2400E+01
Fqi89, tswF5,  170441.906,  235515.672,    1049.174,  0.1625E-01,  0.9277E+01,  0.3271E+02,  0.2552E+01
Fqi90, tswF5,  170698.688,  235432.234,    1049.174,  0.1627E-01,  0.9268E+01,  0.3262E+02,  0.2549E+01
Fsi91, tswF5,  170955.469,  235348.797,    1049.174,  0.2075E-01,  0.3861E+02,  0.1903E+02,  0.2044E+01
Fqi92, tswF5,  171212.266,  235265.375,    1049.174,  0.1738E-01,  0.1429E+02,  0.2771E+02,  0.2385E+01
Fqi93, tswF5,  170466.922,  235592.703,    1048.011,  0.1865E-01,  0.2178E+02,  0.2365E+02,  0.2235E+01
Fri94, tswF5,  170723.719,  235509.266,    1048.011,  0.1751E-01,  0.1499E+02,  0.2722E+02,  0.2367E+01
Fri95, tswF5,  170980.500,  235425.844,    1048.011,  0.1787E-01,  0.1689E+02,  0.2600E+02,  0.2323E+01
Fni96, tswF5,  171237.281,  235342.406,    1048.011,  0.1585E-01,  0.7722E+01,  0.3497E+02,  0.2623E+01
Foi97, tswF6,  170491.953,  235669.734,    1046.849,  0.1945E-01,  0.4177E+02,  0.1702E+02,  0.1684E+01
Fsi98, tswF5,  170748.750,  235586.312,    1046.849,  0.1682E-01,  0.1160E+02,  0.2999E+02,  0.2463E+01
Fqi99, tswF5,  171005.531,  235502.875,    1046.849,  0.1600E-01,  0.8260E+01,  0.3410E+02,  0.2596E+01
Foj 0, tswF6,  170516.984,  235746.781,    1045.686,  0.1721E-01,  0.2042E+02,  0.2231E+02,  0.1881E+01
Fsj 1, tswF5,  170773.766,  235663.344,    1045.686,  0.1964E-01,  0.2897E+02,  0.2122E+02,  0.2137E+01
Fqj 2, tswF5,  171030.562,  235579.906,    1045.686,  0.1633E-01,  0.9507E+01,  0.3234E+02,  0.2541E+01
Fsj 3, tswF6,  170542.016,  235823.812,    1044.523,  0.1557E-01,  0.1032E+02,  0.2887E+02,  0.2091E+01
Fsj 4, tswF5,  170798.797,  235740.375,    1044.523,  0.1649E-01,  0.1014E+02,  0.3154E+02,  0.2514E+01
Frj 5, tswF5,  171312.375,  235573.516,    1044.523,  0.1595E-01,  0.8139E+01,  0.3435E+02,  0.2604E+01
Foj22, tswF5,  170734.109,  230966.938,    1109.983,  0.1373E-01,  0.2344E+01,  0.5478E+02,  0.3153E+01
Fnj23, tswF6,  170794.109,  230967.219,    1109.713,  0.1149E-01,  0.3166E+00,  0.1082E+03,  0.3594E+01
Fnj24, tswF6,  170793.547,  231057.781,    1108.479,  0.1149E-01,  0.3180E+00,  0.1079E+03,  0.3589E+01
Fnj25, tswF5,  170733.859,  231051.609,    1108.828,  0.1405E-01,  0.2898E+01,  0.5044E+02,  0.3048E+01
Foj26, tswF5,  170725.234,  231135.047,    1107.727,  0.1423E-01,  0.3269E+01,  0.4840E+02,  0.2997E+01
Fnj27, tswF5,  170784.922,  231141.219,    1107.378,  0.1193E-01,  0.4202E+00,  0.1058E+03,  0.4130E+01
Fnj28, tswF5,  170716.609,  231218.484,    1106.626,  0.1613E-01,  0.8740E+01,  0.3339E+02,  0.2574E+01
Fnj29, tswF5,  170776.281,  231224.656,    1106.277,  0.1235E-01,  0.7140E+00,  0.8686E+02,  0.3809E+01
Fpj30, tswF5,  170767.812,  231305.531,    1105.210,  0.1322E-01,  0.1580E+01,  0.6358E+02,  0.3352E+01
Foj31, tswF5,  170707.828,  231304.500,    1105.491,  0.1586E-01,  0.7767E+01,  0.3489E+02,  0.2621E+01
Fpj32, tswF5,  170766.797,  231352.031,    1104.580,  0.1528E-01,  0.5821E+01,  0.3876E+02,  0.2736E+01
Foj33, tswF5,  170707.109,  231358.125,    1104.762,  0.1761E-01,  0.1551E+02,  0.2687E+02,  0.2355E+01
Fqj34, tswF5,  170716.469,  231449.906,    1103.467,  0.2270E-01,  0.6003E+02,  0.1610E+02,  0.1909E+01
Fqj35, tswF5,  170776.156,  231443.812,    1103.285,  0.1847E-01,  0.2053E+02,  0.2415E+02,  0.2254E+01
Fqj36, tswF5,  170725.828,  231541.688,    1102.172,  0.1879E-01,  0.2259E+02,  0.2327E+02,  0.2220E+01
Fpj37, tswF5,  170785.516,  231535.609,    1101.991,  0.1453E-01,  0.4031E+01,  0.4511E+02,  0.2912E+01
Fpj38, tswF5,  170735.172,  231633.469,    1100.878,  0.1797E-01,  0.1751E+02,  0.2566E+02,  0.2311E+01
Fpj39, tswF5,  170794.875,  231627.391,    1100.696,  0.1216E-01,  0.5615E+00,  0.9487E+02,  0.3950E+01
Fpj40, tswF5,  170744.531,  231725.250,    1099.583,  0.1832E-01,  0.1965E+02,  0.2459E+02,  0.2271E+01
Fpj41, tswF5,  170804.219,  231719.172,    1099.401,  0.1230E-01,  0.6342E+00,  0.8874E+02,  0.3843E+01
Fqj42, tswF5,  170753.891,  231817.047,    1098.288,  0.1951E-01,  0.2764E+02,  0.2151E+02,  0.2149E+01
Fpj43, tswF5,  170813.578,  231810.953,    1098.107,  0.1326E-01,  0.1650E+01,  0.6284E+02,  0.3336E+01
Fqj44, tswF5,  170998.375,  233694.984,    1071.564,  0.1837E-01,  0.1992E+02,  0.2442E+02,  0.2264E+01
Fqj45, tswF4,  171052.344,  233721.219,    1070.966,  0.1747E-01,  0.4982E+01,  0.1958E+02,  0.1706E+01
Fpj46, tswF4,  171091.516,  233640.625,    1071.893,  0.1994E-01,  0.1067E+02,  0.1471E+02,  0.1517E+01
Frj47, tswF4,  171037.547,  233614.391,    1072.490,  0.2336E-01,  0.2335E+02,  0.1095E+02,  0.1344E+01
Fqj48, tswF4,  171130.688,  233560.031,    1072.820,  0.1589E-01,  0.2795E+01,  0.2483E+02,  0.1880E+01
Frj49, tswF4,  171076.734,  233533.797,    1073.417,  0.2550E-01,  0.3611E+02,  0.9433E+01,  0.1264E+01
```

```
Fqj50, tswF4,  171169.859,  233479.438,    1073.746,  0.1801E-01,  0.6348E+01,  0.1826E+02,  0.1658E+01
Fqj51, tswF4,  171115.906,  233453.203,    1074.344,  0.2264E-01,  0.2030E+02,  0.1157E+02,  0.1375E+01
Foj52, tswF4,  171156.062,  233370.750,    1075.291,  0.2202E-01,  0.1843E+02,  0.1217E+02,  0.1403E+01
Fpj53, tswF4,  171208.062,  233400.703,    1074.652,  0.1919E-01,  0.9134E+01,  0.1591E+02,  0.1567E+01
Fpj54, tswF4,  171209.062,  233285.469,    1076.220,  0.2311E-01,  0.2371E+02,  0.1115E+02,  0.1354E+01
Flj86, tswF5,  171060.891,  235667.781,    1044.351,  0.1796E-01,  0.1747E+02,  0.2571E+02,  0.2312E+01
Fqj87, tswF5,  171201.781,  235578.328,    1044.948,  0.1749E-01,  0.1488E+02,  0.2732E+02,  0.2371E+01
Foj88, tswF5,  171153.562,  235542.625,    1045.649,  0.1918E-01,  0.2567E+02,  0.2229E+02,  0.2181E+01
Fqj89, tswF5,  171294.438,  235453.156,    1046.246,  0.1398E-01,  0.2768E+01,  0.5138E+02,  0.3072E+01
Fnj90, tswF5,  171246.219,  235417.469,    1046.947,  0.1582E-01,  0.7515E+01,  0.3515E+02,  0.2629E+01
Fqk23, tswF5,  170985.000,  234837.000,    1056.031,  0.1675E-01,  0.1126E+02,  0.3031E+02,  0.2474E+01
Fsk26, tswF5,  170347.000,  233659.000,    1074.945,  0.2612E-01,  0.1126E+03,  0.1269E+02,  0.1731E+01
Fpk31, tswF5,  171058.000,  231317.000,    1103.766,  0.1227E-01,  0.6355E+00,  0.9027E+02,  0.3870E+01
Ftk32, tswF6,  170268.000,  232413.000,    1092.307,  0.1612E-01,  0.1320E+02,  0.2628E+02,  0.2012E+01
Fpk33, tswF4,  171234.000,  234074.000,    1065.344,  0.1558E-01,  0.2413E+01,  0.2623E+02,  0.1923E+01
Fnk34, tswF5,  170723.000,  235087.000,    1053.780,  0.2051E-01,  0.3636E+02,  0.1947E+02,  0.2063E+01
Fqk45, tswF4,  171244.422,  233777.672,    1069.344,  0.1985E-01,  0.1099E+02,  0.1484E+02,  0.1523E+01
Fok55, tswF5,  170752.594,  235159.781,    1052.655,  0.1815E-01,  0.1887E+02,  0.2510E+02,  0.2290E+01
Fpk56, tswF5,  170708.016,  235024.562,    1054.699,  0.1592E-01,  0.8302E+01,  0.3452E+02,  0.2610E+01
Fok57, tswF5,  171001.000,  234899.766,    1055.103,  0.1548E-01,  0.6533E+01,  0.3729E+02,  0.2693E+01
Fqk58, tswF5,  170969.156,  234764.547,    1057.090,  0.2024E-01,  0.3401E+02,  0.1997E+02,  0.2085E+01
Fsk59, tswF5,  170268.516,  233672.453,    1075.109,  0.1634E-01,  0.9603E+01,  0.3228E+02,  0.2539E+01
Fsk60, tswF5,  170351.328,  233745.266,    1073.748,  0.2265E-01,  0.5923E+02,  0.1617E+02,  0.1912E+01
Ftk61, tswF5,  170319.484,  233610.047,    1075.735,  0.1706E-01,  0.1282E+02,  0.2899E+02,  0.2429E+01
FoC10, tswFf,  170764.109,  230967.078,    1109.848,  0.1065E-01,  0.3439E+00,  0.3526E+03,  0.2297E+02
FnC11, tswFf,  170763.703,  231054.688,    1108.653,  0.1068E-01,  0.3801E+00,  0.3386E+03,  0.2251E+02
FoC12, tswFf,  170755.078,  231138.125,    1107.552,  0.1077E-01,  0.5159E+00,  0.2971E+03,  0.2109E+02
FnC13, tswFf,  170746.453,  231221.578,    1106.452,  0.1095E-01,  0.8259E+00,  0.2423E+03,  0.1905E+02
FpC14, tswFf,  170737.812,  231305.016,    1105.350,  0.1213E-01,  0.5415E+01,  0.1082E+03,  0.1273E+02
FpC15, tswFf,  170736.953,  231355.078,    1104.671,  0.1377E-01,  0.2059E+02,  0.6109E+02,  0.9562E+01
FqC16, tswFf,  170746.312,  231446.859,    1103.376,  0.1426E-01,  0.2744E+02,  0.5398E+02,  0.8989E+01
FqC17, tswFf,  170755.672,  231538.641,    1102.082,  0.1296E-01,  0.1173E+02,  0.7773E+02,  0.1079E+02
FpC18, tswFf,  170765.016,  231630.438,    1100.787,  0.1122E-01,  0.1483E+01,  0.1881E+03,  0.1678E+02
FpC19, tswFf,  170774.375,  231722.219,    1099.492,  0.1271E-01,  0.9582E+01,  0.8483E+02,  0.1127E+02
FpC20, tswFf,  170783.734,  231814.000,    1098.198,  0.1378E-01,  0.2075E+02,  0.6092E+02,  0.9550E+01
FqC21, tswFf,  171025.359,  233708.094,    1071.265,  0.1345E-01,  0.1680E+02,  0.6670E+02,  0.9992E+01
FqC22, tswFf,  171064.531,  233627.500,    1072.192,  0.1365E-01,  0.1921E+02,  0.6301E+02,  0.9711E+01
FrC23, tswFf,  171103.703,  233546.906,    1073.118,  0.1266E-01,  0.9129E+01,  0.8665E+02,  0.1139E+02
FqC24, tswFf,  171142.891,  233466.312,    1074.045,  0.1354E-01,  0.1784E+02,  0.6506E+02,  0.9868E+01
FpC25, tswFf,  171182.062,  233385.719,    1074.972,  0.1290E-01,  0.1125E+02,  0.7931E+02,  0.1090E+02
FnC41, tswFf,  171085.016,  235685.641,    1044.001,  0.1290E-01,  0.1141E+02,  0.7936E+02,  0.1090E+02
FoC42, tswFf,  171177.672,  235560.469,    1045.299,  0.1294E-01,  0.1149E+02,  0.7836E+02,  0.1083E+02
FqC43, tswFf,  171270.328,  235435.312,    1046.596,  0.1187E-01,  0.4004E+01,  0.1232E+03,  0.1358E+02
total area of repository (m^2) =  0.49017E+07
total kg/s over repository =  0.30314E+01
average mm/year over repository =  0.19503E+02
```

I.3 Source File for T2WEEP v. 1.0

```
c     program t2weep_v1.f
c_____________________________________________________________________
c  This program will extract incoming percolation and discrete weep
c  spacings for repository elements that are prescribed by the user.
c  The LBNL 3-D TOUGH2 UZ flow field and mesh are used as input, and a
c  file is created that contains the element, coordinates, percolation
c  flux (mm/year), and weep spacings (using two methods described
c  below).
c
c  1) Read in user-prescribed files and data (Sfr, gamma for repository
c     units, Afm/V parameters, liquid density etc.)
c  2) Read in repository elements from user-prescribed file
c  3) Read in element information (name, material, coordiates) from
c     ELEME and assign parameter values to repository elements based on
c     material type. Record element name directly above repository
c     element to identify appropriate connections.
c  4) Read in connection information from CONNE card for connections
c     identified in step 3.  Record connection area for those connections.
c  5) Read TOUGH2 output file prescribed by user.  First read in
c     liquid saturations for prescribed repository elements. Then
c     read in mass flow rates for those connections identified in step 3.
c  6) Calculate percolation flux from mass flow using connection area
c     and liquid density.
c  7) Calculate weep spacing using two methods:  (a) assume active
c     fractures are saturated and use Xfm=Sfe, and
c     (b) fractures are unsaturated where active weep spacing is
c     calculated from Liu et al. (1998) using da=d/Se^gamma.
c  8) Print results to output file.
c
c  C.K.Ho 11/19/99
c_____________________________________________________________________
c234567890123456789012345678901234567890123456789012345678901234567890123456789012
c     implicit double precision (a-h,o-z)

      dimension x(1001),y(1001),z(1001),area(1001),sl(1001),gamma(1001)
      real  ml(1001),a(1001),d(1001)
      character*100 block,output,t2out,t2mesh,repo
      character*5 elemr(1001),mat(1001),elemr1(1001),elemr2(1001)
      character*5 elem1,elem2,elemold

c_____________________________________________________________________
c  1) Read in user-prescribed files and data (Sfr, gamma for repository
c     units, Afm/V parameters, liquid density etc.)
c_____________________________________________________________________
      write(*,*)'What is the name of repository element file?'
      read(*,'(a)') repo
      write(*,*) 'What is the name of the TOUGH2 output file?'
      read(*,'(a)') t2out
      write(*,*) 'What is the name of the TOUGH2 mesh file?'
      read(*,'(a)') t2mesh
      write(*,*) 'What would you like to name your output file?'
      read(*,'(a)') output
      write(*,*)'What is the residual fracture liquid saturation?'
      read(*,*) sfr
      write(*,*)'What is the liquid density (kg/m^3)?'
      read(*,*) rho
      write(*,*)'What are the gamma parameters for the units:'
      write(*,*)'tswF4, tswF5, tswF6, and tswFf?'
      read(*,*) g4,g5,g6,gf
      write(*,*)'What are the (Afm/V) parameters for the units:'
      write(*,*)'tswF4, tswF5, tswF6, and tswFf?'
      read(*,*) afm4,afm5,afm6,afmf
      write(*,*)'Geometric fracture spacings (m) for the units:'
      write(*,*)'tswF4, tswF5, tswF6, and tswFf?'
      read(*,*) d4,d5,d6,df
```

```
      open(1,file=t2mesh,status='old')
      open(2,file=t2out,status='old')
      open(3,file=repo,status='old')
      open(4,file=output,status='unknown')

c...Data
      mm_per_m=1000
      sec_per_year=3.1536e7

c...Write header information to output file
      write(4,25) t2out,t2mesh,repo,g4,g5,g6,gf,afm4,afm5,afm6,afmf,
     &            d4,d5,d6,df
25    format('*** Output file from t2weep_v1.f ***',/
     & 'TOUGH2 output file: ',a,/
     & 'TOUGH2 mesh file: ',a,/
     & 'Repository element file: ',a,/
     & 'Gamma value for tswF4, tswF5, tswF6, and tswFf: ',4f7.2,/
     & 'Afm/V value for tswF4, tswF5, tswF6, and tswFf: ',4f7.2,/
     & 'Fracture spacing for tswF4, tswF5, tswF6, and tswFf: ',4f7.2,/
     & 'The percolation flux is that entering the listed repository '/
     & 'element from the element above. The first weep spacing '/
     & 'assumes that the fractures with weeps are saturated '/
     & '(i.e., weep width in each fracture equals weep spacing).'/
     & 'The second weep spacing assumes that the active fractures '/
     & 'are unsaturated and is taken from eq. 17 of Liu et al. '/
     & '(1998) WRR, 34(10), 2633-2646.'/
     & '***Note that fault materials (ending in "f") are placed '
     & 'at the end of the file***'//
     & 'Element, material, x(m), y(m), z(m), Sl, '
     & 'percolation(mm/year), weep_spacing1(m), weep_spacing2(m)')

c_____________________________________________________________________
c  2) Read in repository elements from user-prescribed file
c_____________________________________________________________________
      read(3,*) nrepo
      read(3,'(a)') (elemr(i),i=1,nrepo)

c_____________________________________________________________________
c  3) Read in element information (name, material, coordiates) from
c     ELEME and assign parameter values to repository elements based on
c     material type. Record element name directly above repository
c     element to identify appropriate connections.
c_____________________________________________________________________
c...Read in element information from ELEME
c...N is the counter on all elements
c...i is the counter on just repository elements
      N=1
      i=1
      READ(1,1000) BLOCK
1000  FORMAT(A22,28X,3f10.3)
99    READ(1,1000) BLOCK,xx,yy,zz
      IF(BLOCK(1:5).EQ.'     ') GO TO 98
      if(block(1:5).ne.elemr(i)) then
c...Remember name of previously read element
        elemold=block(1:5)
        elemold(1:1)='F'
        n=n+1
        go to 99
      end if
c...If a repository element is read, designate element 1 as the
c...repository element and element 2 as the previous element read (which
c...will be the element directly above it). mat(i) is the material type.
      elemr1(i) = elemr(i)
      elemr2(i) = elemold
      mat(i)=block(16:20)
      x(i)=xx
      y(i)=yy
      z(i)=zz
c...Assign gamma value based on material of element.
      if(mat(i).eq.'tswF4') then
```

```
        gamma(i)=g4
        a(i)=afm4
        d(i)=d4
      elseif(mat(i).eq.'tswF5') then
        gamma(i)=g5
        a(i)=afm5
        d(i)=d5
      elseif(mat(i).eq.'tswF6') then
        gamma(i)=g6
        a(i)=afm6
        d(i)=d6
      elseif(mat(i).eq.'tswFf') then
        gamma(i)=gf
        a(i)=afmf
        d(i)=df
      else
        write(*,*) '***Could not match repository materials!***'
      end if
c...If the element is a fracture, subtract 0.5 m from the
c...x-coordinate because LBNL adds 0.5 m for fracture-matrix interactions
      if(elemr1(i)(1:1).eq.'F') x(i)=x(i)-0.5
      i=i+1
      n=n+1
      GO TO 99
98    CONTINUE
      NMAX = N - 1
      nmaxr=i-1

      write(*,50) nmax,nmaxr
50    format('Have read in ',i6,' elements in ELEME and'/
     &        i6,' repository elements in ELEME...')

c_______________________________________________________________________
c  4) Read in connection information from CONNE card for connections
c     identified in step 3.  Record connection area for those connections.
c_______________________________________________________________________
c...N is the counter on all connections
c...i is the counter on just repository connections
      N=1
      i=1
      areatot=0.
      READ(1,1500) BLOCK
1500  FORMAT(A22,3X,I5,20X,E10.4)
199   READ(1,1500) BLOCK,isot,areax
      IF(BLOCK(1:5).EQ.'     '.OR.BLOCK(1:3).EQ.'+++') GO TO 198
      elem1 = BLOCK(1:5)
      elem2 = BLOCK(6:10)
      if(elem1.eq.elemr1(i).and.elem2.eq.elemr2(i)) then
        area(i)=areax
        areatot=areatot+areax
        i=i+1
      end if
      N=N+1
      GO TO 199
198   CONTINUE
      NCMAX = N - 1
4000  CONTINUE

      write(*,197) ncmax,i-1
197   format('Have read in ',i6,' number of connections',/
     &       'and ',i6,' number of repository connections...')

c_______________________________________________________________________
c  5) Read TOUGH2 output file prescribed by user.  First read in
c     liquid saturations for prescribed repository elements. Then
c     read in mass flow rates for those connections identified in step 4.
c_______________________________________________________________________
89    READ(2,1000,END=90) BLOCK
      IF(BLOCK(1:12).NE.'  TOTAL TIME') GO TO 89
      READ(2,1001) TIME
1001  FORMAT(E13.4)
```

```
      do i=1,6
        READ(2,1000) BLOCK
      end do
c...Read in liquid saturations from TOUGH2 output file.  If element is
c...a repository element, record liquid saturation.
      i=1
      N1=1
      N2=MIN(NMAX,45)
      DO 2000 n=N1,N2
      READ(2,1002) elem1,slx
1002  FORMAT(1x,a5,24x,e12.5)
      if(elem1.eq.elemr(i)) then
        sl(i)=slx
        i=i+1
      end if
2000  CONTINUE
C
2100  CONTINUE
      IF(N2.EQ.NMAX) GO TO 91
      N1=N2+1
      N2=MIN(NMAX,N1+56)
      do j=1,3
        READ(2,1000) BLOCK
      end do
      DO 2010 n=N1,N2
      READ(2,1002) elem1,slx
      if(elem1.eq.elemr(i)) then
        sl(i)=slx
        i=i+1
      end if
2010  CONTINUE
      GO TO 2100
C
91    CONTINUE
C
      write(*,149)i-1
149   format('Have read in ',i6,' repository liquid saturations...')

c...Read in mass flow rates from TOUGH2 output file
      i=1
      flotot=0.
289   READ(2,1500,END=190) BLOCK
      IF(BLOCK(7:18).NE.'ELEM1  ELEM2') GO TO 289
      READ(2,1500) BLOCK
      READ(2,1500) BLOCK
C
      N1=1
      N2=MIN(NCMAX,53)
      DO 1600 n=N1,N2
      READ(2,1003) block,flow
1003  FORMAT(a32,E12.5)
      elem1=block(6:10)
      elem2=block(15:19)
      if(elem1.eq.elemr1(i).and.elem2.eq.elemr2(i))then
        ml(i)=flow
        flotot=flotot+flow
        i=i+1
      end if
1600  CONTINUE
C
2150  CONTINUE
      IF(N2.EQ.NCMAX) GO TO 191
      N1=N2+1
      N2=MIN(NCMAX,N1+56)
      do j=1,3
        READ(2,1500) BLOCK
      end do
      DO 2020 n=N1,N2
      READ(2,1003) block,flow
      elem1=block(6:10)
      elem2=block(15:19)
```

```
      if(elem1.eq.elemr1(i).and.elem2.eq.elemr2(i))then
        ml(i)=flow
        flotot=flotot+flow
        i=i+1
      end if
2020  CONTINUE
      GO TO 2150
C
191   CONTINUE
C
190   CONTINUE
      write(*,174)i-1
174   format('Have read in ',i6,' repository fluxes...')

c...Loop through all repository elements and calculate percolation
c...flux (darcy velocity in mm/year) and weep spacing using two methods.
c...Print results to output file

      do i=1,nrepo
c_______________________________________________________________________
c  6) Calculate percolation flux (mm/year) from mass flow using
c     connection area and liquid density.
c_______________________________________________________________________
        perc=ml(i)/area(i)/rho*mm_per_m*sec_per_year

c...Calculate effective saturation, se
        se=(sl(i)-sfr)/(1-sfr)

c_______________________________________________________________________
c  7) Calculate weep spacing using two methods:  (a) assume active
c     fractures are saturated and use Xfm=Sfe, and
c     (b) fractures are unsaturated where active weep spacing is
c     calculated from Liu et al. (1998) using da=d/Se^gamma.
c_______________________________________________________________________
c...Calculate weep_spacing1 (m)
        weep1=2./se/a(i)

c...Calculate weep_spacing2 (m)
        weep2=d(i)/se**gamma(i)

c_______________________________________________________________________
c  8) Print results to output file.
c_______________________________________________________________________
        if(mat(i)(5:5).ne.'f') then
          write(4,82) elemr(i),mat(i),x(i),y(i),z(i),sl(i),
     &              perc,weep1,weep2
82        format(2(a5,', '),3(f11.3,', '),3(e11.4,', '),e11.4)
        end if

      end do

c...Print all fault materials at the end of the file in case the
c...user does not want to include those in the distribution
      do i=1,nrepo
        perc=ml(i)/area(i)/rho*mm_per_m*sec_per_year
        se=(sl(i)-sfr)/(1-sfr)
        weep1=2./se/a(i)
        weep2=d(i)/se**gamma(i)
        if(mat(i)(5:5).eq.'f') then
          write(4,82) elemr(i),mat(i),x(i),y(i),z(i),sl(i),
     &              perc,weep1,weep2
        end if
      end do

c...Print out average percolation flux over entire repository area
      percavg=flotot/areatot/rho*mm_per_m*sec_per_year
      write(4,94) areatot,flotot,percavg
94    format('total area of repository (m^2) = ',e12.5/
     &       'total kg/s over repository = ',e12.5/
     &       'average mm/year over repository = ',e12.5)
```

```
90    CONTINUE
C
      stop
      end
```

ATTACHMENT II

Repository Elements

Figure II-1 shows the location of the repository elements that are listed in Table II-1. This plot verifies that the elements fall within the boundaries of the repository outline(the segments for the repository outline were obtained from DTN: SN9907T0872799.001). Figure II-2 shows the elevation of the repository elements as a function of the northing direction. Note that they all fall between elevations of 1040 m and 1120 m.

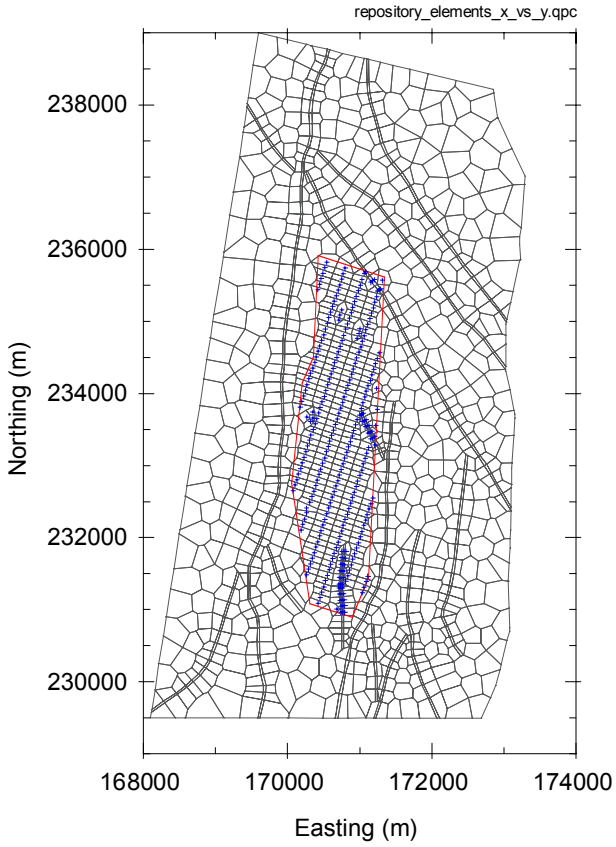

Figure II-1. Prescribed Repository Elements.
Symbols denote location of 275 repository elements (see Table II-1) relative to the outline of the repository (DTN: SN9907T0872799.001).

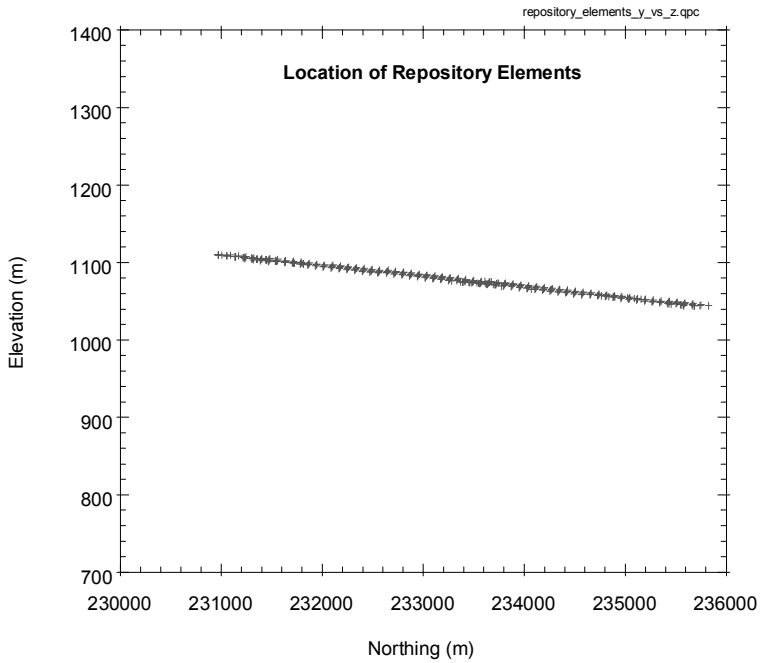

Figure II-2. Elevation of the 275 Repository Elements Along the Northing Coordinate

Table II-1. 275 Fracture Elements Denoted as Repository Elements (taken from 3d2kpa_pc1.mesh; DTN: LB990701233129.001).

Fracture Element	Material	Volume	x (m)	y (m)	z (m)
Fph 2	tswF6	3.23E+03	170424.8	231092.6	1109.641
Foh 3	tswF5	1.00E+03	170681.6	231009.2	1109.641
Fph 4	tswF6	1.64E+03	170449.8	231169.7	1108.478
Foh 5	tswF6	1.53E+03	170474.9	231246.7	1107.315
Fph 6	tswF6	1.50E+03	170499.9	231323.8	1106.152
Fsh 7	tswF6	2.17E+03	170268.1	231484.2	1104.99
Fph 8	tswF6	1.41E+03	170524.9	231400.8	1104.99
Fph 9	tswF5	1.49E+03	171038.5	231233.9	1104.99
Fsh10	tswF6	1.22E+03	170293.2	231561.3	1103.827
Fqh11	tswF5	1.02E+03	170550	231477.8	1103.827
Fqh12	tswF5	7.82E+02	170806.7	231394.4	1103.827
Fsh13	tswF6	1.55E+03	170318.2	231638.3	1102.664
Fph14	tswF5	8.98E+02	170575	231554.9	1102.664
Fqh15	tswF5	6.99E+02	170831.8	231471.4	1102.664
Foh16	tswF5	9.29E+02	171088.6	231388	1102.664
Frh17	tswF6	1.90E+03	170343.2	231715.3	1101.501
Fph18	tswF5	9.08E+02	170600	231631.9	1101.501
Fph19	tswF5	7.65E+02	170856.8	231548.5	1101.501
Foh20	tswF5	1.80E+03	171113.6	231465	1101.501
Frh21	tswF6	1.80E+03	170368.3	231792.4	1100.338
Fph22	tswF5	8.69E+02	170625	231708.9	1100.338
Fph23	tswF5	8.63E+02	170881.8	231625.5	1100.338
Fsh24	tswF6	1.72E+03	170393.3	231869.4	1099.175
Fph25	tswF5	8.36E+02	170650.1	231786	1099.175
Foh26	tswF5	9.12E+02	170906.9	231702.5	1099.175
Frh27	tswF5	1.32E+03	170418.3	231946.4	1098.013
Fph28	tswF5	8.09E+02	170675.1	231863	1098.013
Foh29	tswF5	8.63E+02	170931.9	231779.6	1098.013
Fth30	tswF6	3.06E+03	170186.6	232106.9	1096.85
Fsh31	tswF5	1.21E+03	170443.3	232023.5	1096.85
Fph32	tswF5	1.05E+03	170700.1	231940	1096.85
Foh33	tswF5	1.04E+03	170956.9	231856.6	1096.85
Fuh34	tswF6	1.73E+03	170211.6	232183.9	1095.687
Fqh35	tswF5	1.21E+03	170468.4	232100.5	1095.687
Fph36	tswF5	1.19E+03	170725.2	232017.1	1095.687
Foh37	tswF5	1.40E+03	170981.9	231933.6	1095.687
Fth38	tswF6	1.68E+03	170236.6	232261	1094.524
Fqh39	tswF5	1.21E+03	170493.4	232177.5	1094.524
Fph40	tswF5	1.21E+03	170750.2	232094.1	1094.524
Foh41	tswF5	1.26E+03	171007	232010.7	1094.524
Fth42	tswF6	1.45E+03	170261.6	232338	1093.361
Fqh43	tswF5	1.31E+03	170518.4	232254.6	1093.361
Fph44	tswF5	1.21E+03	170775.2	232171.1	1093.361
Foh45	tswF5	1.29E+03	171032	232087.7	1093.361
Fqh46	tswF5	1.01E+03	170543.5	232331.6	1092.199

Fracture Element	Material	Volume	x (m)	y (m)	z (m)
Fph47	tswF5	1.21E+03	170800.2	232248.2	1092.199
Foh48	tswF5	1.06E+03	171057	232164.8	1092.199
Fth49	tswF5	1.30E+03	170311.7	232492.1	1091.036
Frh50	tswF5	1.32E+03	170568.5	232408.6	1091.036
Fqh51	tswF5	1.21E+03	170825.3	232325.2	1091.036
Foh52	tswF5	8.03E+02	171082.1	232241.8	1091.036
Fmh53	tswF6	2.40E+03	170079.9	232652.5	1089.873
Fth54	tswF5	1.21E+03	170336.7	232569.1	1089.873
Fqh55	tswF5	1.21E+03	170593.5	232485.7	1089.873
Fph56	tswF5	1.21E+03	170850.3	232402.3	1089.873
Foh57	tswF5	8.91E+02	171107.1	232318.8	1089.873
Frh58	tswF6	1.42E+03	170105	232729.6	1088.71
Fth59	tswF5	1.21E+03	170361.8	232646.2	1088.71
Fqh60	tswF5	1.21E+03	170618.5	232562.7	1088.71
Frh61	tswF5	1.21E+03	170875.3	232479.3	1088.71
Foh62	tswF5	1.13E+03	171132.1	232395.9	1088.71
Fph63	tswF6	1.37E+03	170130	232806.6	1087.547
Fth64	tswF5	1.21E+03	170386.8	232723.2	1087.547
Fqh65	tswF5	1.21E+03	170643.6	232639.8	1087.547
Fqh66	tswF5	1.21E+03	170900.4	232556.3	1087.547
Foh67	tswF4	9.56E+02	171157.2	232472.9	1087.547
Fmh68	tswF6	1.75E+03	170155	232883.7	1086.384
Fth69	tswF5	1.21E+03	170411.8	232800.2	1086.384
Frh70	tswF5	1.21E+03	170668.6	232716.8	1086.384
Fqh71	tswF5	1.21E+03	170925.4	232633.4	1086.384
Foh72	tswF4	1.52E+03	171182.2	232549.9	1086.384
Frh73	tswF5	1.07E+03	170180.1	232960.7	1085.222
Fsh74	tswF5	1.21E+03	170436.9	232877.3	1085.222
Frh75	tswF5	1.21E+03	170693.6	232793.8	1085.222
Frh76	tswF5	1.16E+03	170950.4	232710.4	1085.222
Frh77	tswF5	1.16E+03	170205.1	233037.7	1084.059
Fsh78	tswF5	1.21E+03	170461.9	232954.3	1084.059
Fqh79	tswF5	1.21E+03	170718.7	232870.9	1084.059
Fph80	tswF5	1.30E+03	170975.5	232787.4	1084.059
Fsh81	tswF5	1.01E+03	170230.1	233114.8	1082.896
Fsh82	tswF5	1.21E+03	170486.9	233031.3	1082.896
Fqh83	tswF5	1.21E+03	170743.7	232947.9	1082.896
Foh84	tswF5	1.21E+03	171000.5	232864.5	1082.896
Fsh85	tswF5	9.93E+02	170255.2	233191.8	1081.733
Fsh86	tswF5	1.21E+03	170511.9	233108.4	1081.733
Fqh87	tswF5	1.21E+03	170768.7	233024.9	1081.733
Fph88	tswF5	1.30E+03	171025.5	232941.5	1081.733
Fsh89	tswF5	1.21E+03	170280.2	233268.8	1080.57
Fsh90	tswF5	1.21E+03	170537	233185.4	1080.57
Fqh91	tswF5	1.21E+03	170793.8	233102	1080.57
Foh92	tswF5	1.30E+03	171050.5	233018.5	1080.57
Fth93	tswF5	1.13E+03	170305.2	233345.9	1079.408
Fsh94	tswF5	1.21E+03	170562	233262.4	1079.408
Fqh95	tswF5	1.21E+03	170818.8	233179	1079.408
Foh96	tswF5	1.19E+03	171075.6	233095.6	1079.408

Fracture Element	Material	Volume	x (m)	y (m)	z (m)
Fth97	tswF5	1.30E+03	170330.2	233422.9	1078.245
Fsh98	tswF5	1.21E+03	170587	233339.5	1078.245
Fph99	tswF5	1.21E+03	170843.8	233256	1078.245
Foi 0	tswF4	9.33E+02	171100.6	233172.6	1078.245
Fsi 1	tswF5	8.75E+02	170355.3	233499.9	1077.082
Fsi 2	tswF5	1.21E+03	170612.1	233416.5	1077.082
Fqi 3	tswF5	1.33E+03	170868.8	233333.1	1077.082
Foi 4	tswF4	8.81E+02	171125.6	233249.6	1077.082
Fsi 5	tswF5	7.34E+02	170380.3	233577	1075.919
Fsi 6	tswF5	1.21E+03	170637.1	233493.5	1075.919
Fsi 7	tswF5	1.03E+03	170893.9	233410.1	1075.919
Fsi 8	tswF5	7.45E+02	170405.3	233654	1074.756
Fsi 9	tswF5	1.21E+03	170662.1	233570.6	1074.756
Fqi10	tswF5	1.02E+03	170918.9	233487.2	1074.756
Fri11	tswF5	1.57E+03	170173.6	233814.5	1073.593
Fsi12	tswF5	1.01E+03	170430.4	233731	1073.593
Fri13	tswF5	1.21E+03	170687.1	233647.6	1073.593
Fri14	tswF5	8.80E+02	170943.9	233564.2	1073.593
Fri15	tswF5	1.22E+03	170198.6	233891.5	1072.431
Fsi16	tswF5	9.81E+02	170455.4	233808.1	1072.431
Fri17	tswF5	1.27E+03	170712.2	233724.7	1072.431
Fqi18	tswF5	7.21E+02	170969	233641.2	1072.431
Fqi19	tswF4	9.15E+02	171225.7	233557.8	1072.431
Fsi20	tswF5	1.14E+03	170223.6	233968.6	1071.268
Fsi21	tswF5	1.21E+03	170480.4	233885.1	1071.268
Fri22	tswF5	1.06E+03	170737.2	233801.7	1071.268
Fsi23	tswF5	1.46E+03	170248.7	234045.6	1070.105
Fsi24	tswF5	1.21E+03	170505.4	233962.2	1070.105
Fsi25	tswF5	1.31E+03	170762.2	233878.7	1070.105
Fri26	tswF4	8.73E+02	171019	233795.3	1070.105
Fsi27	tswF5	1.26E+03	170273.7	234122.6	1068.942
Fsi28	tswF5	1.21E+03	170530.5	234039.2	1068.942
Fri29	tswF5	1.21E+03	170787.3	233955.8	1068.942
Fri30	tswF4	9.81E+02	171044	233872.3	1068.942
Fsi31	tswF5	1.39E+03	170298.7	234199.7	1067.779
Fsi32	tswF5	1.21E+03	170555.5	234116.2	1067.779
Fri33	tswF5	1.21E+03	170812.3	234032.8	1067.779
Fqi34	tswF4	9.12E+02	171069.1	233949.4	1067.779
Fsi35	tswF5	1.43E+03	170323.7	234276.7	1066.617
Fsi36	tswF5	1.21E+03	170580.5	234193.3	1066.617
Fqi37	tswF5	1.21E+03	170837.3	234109.8	1066.617
Fpi38	tswF4	9.39E+02	171094.1	234026.4	1066.617
Fsi39	tswF5	1.45E+03	170348.8	234353.7	1065.454
Fri40	tswF5	1.21E+03	170605.6	234270.3	1065.454
Fqi41	tswF5	1.21E+03	170862.3	234186.9	1065.454
Fpi42	tswF4	7.90E+02	171119.1	234103.4	1065.454
Fsi43	tswF5	1.46E+03	170373.8	234430.8	1064.291
Fsi44	tswF5	1.21E+03	170630.6	234347.3	1064.291
Fqi45	tswF5	1.21E+03	170887.4	234263.9	1064.291
Fpi46	tswF4	8.00E+02	171144.2	234180.5	1064.291

Fracture Element	Material	Volume	x (m)	y (m)	z (m)
Fsi47	tswF5	1.21E+03	170398.8	234507.8	1063.128
Fri48	tswF5	1.21E+03	170655.6	234424.4	1063.128
Fpi49	tswF5	1.21E+03	170912.4	234340.9	1063.128
Fqi50	tswF4	9.79E+02	171169.2	234257.5	1063.128
Fsi51	tswF5	1.03E+03	170423.9	234584.8	1061.965
Fri52	tswF5	1.21E+03	170680.7	234501.4	1061.965
Fri53	tswF5	1.21E+03	170937.4	234418	1061.965
Fri54	tswF4	9.92E+02	171194.2	234334.5	1061.965
Fsi55	tswF5	1.02E+03	170448.9	234661.9	1060.802
Fsi56	tswF5	1.21E+03	170705.7	234578.4	1060.802
Fri57	tswF5	1.21E+03	170962.5	234495	1060.802
Fqi58	tswF4	1.15E+03	171219.3	234411.6	1060.802
Fsi59	tswF5	1.11E+03	170473.9	234738.9	1059.64
Fri60	tswF5	1.21E+03	170730.7	234655.5	1059.64
Fpi61	tswF5	1.21E+03	170987.5	234572.1	1059.64
Fpi62	tswF4	9.30E+02	171244.3	234488.6	1059.64
Fsi63	tswF5	1.02E+03	170499	234815.9	1058.477
Fri64	tswF5	1.09E+03	170755.7	234732.5	1058.477
Fpi65	tswF5	1.07E+03	171012.5	234649.1	1058.477
Fpi66	tswF4	1.60E+03	171269.3	234565.7	1058.477
Fsi67	tswF5	1.04E+03	170524	234893	1057.314
Fqi68	tswF5	1.24E+03	170780.8	234809.6	1057.314
Foi69	tswF5	1.03E+03	171037.6	234726.1	1057.314
Fqi70	tswF5	9.33E+02	170549	234970	1056.151
Fqi71	tswF5	8.96E+02	170805.8	234886.6	1056.151
Fpi72	tswF5	8.24E+02	171062.6	234803.2	1056.151
Fqi73	tswF5	1.30E+03	170574	235047.1	1054.988
Fpi74	tswF5	1.06E+03	170830.8	234963.6	1054.988
Foi75	tswF5	7.27E+02	171087.6	234880.2	1054.988
Fqi76	tswF5	1.02E+03	170599.1	235124.1	1053.826
Fpi77	tswF5	7.70E+02	170855.9	235040.7	1053.826
Fqi78	tswF5	9.96E+02	171112.6	234957.2	1053.826
Foi79	tswF5	1.07E+03	170624.1	235201.1	1052.663
Fqi80	tswF5	9.12E+02	170880.9	235117.7	1052.663
Fqi81	tswF5	1.05E+03	171137.7	235034.3	1052.663
Fmi82	tswF5	1.14E+03	170649.1	235278.2	1051.5
Fsi83	tswF5	1.06E+03	170905.9	235194.7	1051.5
Fsi84	tswF5	9.90E+02	171162.7	235111.3	1051.5
Fri85	tswF5	1.90E+03	170417.4	235438.6	1050.337
Fqi86	tswF5	1.18E+03	170674.2	235355.2	1050.337
Fsi87	tswF5	1.16E+03	170930.9	235271.8	1050.337
Fsi88	tswF5	1.08E+03	171187.7	235188.3	1050.337
Fqi89	tswF5	1.02E+03	170442.4	235515.7	1049.174
Fqi90	tswF5	1.21E+03	170699.2	235432.2	1049.174
Fsi91	tswF5	1.21E+03	170956	235348.8	1049.174
Fqi92	tswF5	9.19E+02	171212.8	235265.4	1049.174
Fqi93	tswF5	9.19E+02	170467.4	235592.7	1048.011
Fri94	tswF5	1.21E+03	170724.2	235509.3	1048.011
Fri95	tswF5	1.11E+03	170981	235425.8	1048.011
Fni96	tswF5	8.32E+02	171237.8	235342.4	1048.011

Fracture Element	Material	Volume	x (m)	y (m)	z (m)
Foi97	tswF6	1.50E+03	170492.5	235669.7	1046.849
Fsi98	tswF5	1.21E+03	170749.2	235586.3	1046.849
Fqi99	tswF5	1.08E+03	171006	235502.9	1046.849
Foj 0	tswF6	1.67E+03	170517.5	235746.8	1045.686
Fsj 1	tswF5	1.23E+03	170774.3	235663.3	1045.686
Fqj 2	tswF5	9.74E+02	171031.1	235579.9	1045.686
Fsj 3	tswF6	3.56E+03	170542.5	235823.8	1044.523
Fsj 4	tswF5	1.68E+03	170799.3	235740.4	1044.523
Frj 5	tswF5	1.89E+03	171312.9	235573.5	1044.523
FoC10	tswFf	4.73E+02	170764.6	230967.1	1109.848
Foj22	tswF5	2.86E+02	170734.6	230966.9	1109.983
Fnj23	tswF6	9.59E+02	170794.6	230967.2	1109.713
FnC11	tswFf	4.63E+02	170764.2	231054.7	1108.653
Fnj24	tswF6	1.05E+03	170794	231057.8	1108.479
Fnj25	tswF5	2.51E+02	170734.4	231051.6	1108.828
FoC12	tswFf	4.54E+02	170755.6	231138.1	1107.552
Foj26	tswF5	6.53E+02	170725.7	231135	1107.727
Fnj27	tswF5	7.51E+02	170785.4	231141.2	1107.378
FnC13	tswFf	4.53E+02	170746.9	231221.6	1106.452
Fnj28	tswF5	6.38E+02	170717.1	231218.5	1106.626
Fnj29	tswF5	6.72E+02	170776.8	231224.7	1106.277
FpC14	tswFf	3.61E+02	170738.3	231305	1105.351
Fpj30	tswF5	4.45E+02	170768.3	231305.5	1105.21
Foj31	tswF5	5.02E+02	170708.3	231304.5	1105.491
FpC15	tswFf	3.91E+02	170737.5	231355.1	1104.671
Fpj32	tswF5	1.57E+02	170767.3	231352	1104.58
Foj33	tswF5	4.64E+02	170707.6	231358.1	1104.762
FqC16	tswFf	5.07E+02	170746.8	231446.9	1103.376
Fqj34	tswF5	4.85E+02	170717	231449.9	1103.467
Fqj35	tswF5	1.70E+02	170776.7	231443.8	1103.285
FqC17	tswFf	4.99E+02	170756.2	231538.6	1102.082
Fqj36	tswF5	4.76E+02	170726.3	231541.7	1102.172
Fpj37	tswF5	2.29E+02	170786	231535.6	1101.991
FpC18	tswFf	4.99E+02	170765.5	231630.4	1100.787
Fpj38	tswF5	4.02E+02	170735.7	231633.5	1100.878
Fpj39	tswF5	3.02E+02	170795.4	231627.4	1100.696
FpC19	tswFf	4.99E+02	170774.9	231722.2	1099.492
Fpj40	tswF5	3.50E+02	170745	231725.3	1099.583
Fpj41	tswF5	3.18E+02	170804.7	231719.2	1099.401
FpC20	tswFf	7.79E+02	170784.2	231814	1098.198
Fqj42	tswF5	3.63E+02	170754.4	231817	1098.288
Fpj43	tswF5	6.20E+02	170814.1	231811	1098.107
FqC21	tswFf	4.95E+02	171025.9	233708.1	1071.265
Fqj44	tswF5	6.14E+02	170998.9	233695	1071.564
Fqj45	tswF4	4.67E+02	171052.8	233721.2	1070.966
FqC22	tswFf	4.84E+02	171065	233627.5	1072.192
Fpj46	tswF4	4.54E+02	171092	233640.6	1071.893
Frj47	tswF4	2.53E+02	171038.1	233614.4	1072.491
FrC23	tswFf	4.84E+02	171104.2	233546.9	1073.118
Fqj48	tswF4	2.98E+02	171131.2	233560	1072.82

Fracture Element	Material	Volume	x (m)	y (m)	z (m)
Frj49	tswF4	4.19E+02	171077.2	233533.8	1073.417
FqC24	tswFf	4.84E+02	171143.4	233466.3	1074.045
Fqj50	tswF4	3.13E+02	171170.4	233479.4	1073.746
Fqj51	tswF4	6.18E+02	171116.4	233453.2	1074.344
FpC25	tswFf	5.00E+02	171182.6	233385.7	1074.972
Foj52	tswF4	4.83E+02	171156.6	233370.7	1075.291
Fpj53	tswF4	5.10E+02	171208.6	233400.7	1074.652
Fpj54	tswF4	2.49E+02	171209.6	233285.5	1076.221
FnC41	tswFf	9.67E+02	171085.5	235685.6	1044.001
Flj86	tswF5	5.72E+02	171061.4	235667.8	1044.351
FoC42	tswFf	1.13E+03	171178.2	235560.5	1045.299
Fqj87	tswF5	6.83E+02	171202.3	235578.3	1044.948
Foj88	tswF5	7.00E+02	171154.1	235542.6	1045.649
FqC43	tswFf	1.04E+03	171270.8	235435.3	1046.596
Fqj89	tswF5	6.41E+02	171294.9	235453.2	1046.246
Fnj90	tswF5	5.22E+02	171246.7	235417.5	1046.947
Fqk23	tswF5	5.35E+02	170985.5	234837	1056.031
Fsk26	tswF5	2.54E+02	170347.5	233659	1074.945
Fpk31	tswF5	9.90E+02	171058.5	231317	1103.767
Ftk32	tswF6	1.87E+03	170268.5	232413	1092.307
Fpk33	tswF4	8.82E+02	171234.5	234074	1065.344
Fnk34	tswF5	5.74E+02	170723.5	235087	1053.78
Fqk45	tswF4	9.80E+02	171244.9	233777.7	1069.344
Fok55	tswF5	9.14E+02	170753.1	235159.8	1052.655
Fpk56	tswF5	4.06E+02	170708.5	235024.6	1054.699
Fok57	tswF5	8.94E+02	171001.5	234899.8	1055.103
Fqk58	tswF5	4.53E+02	170969.7	234764.5	1057.091
Fsk59	tswF5	9.85E+02	170269	233672.5	1075.109
Fsk60	tswF5	4.64E+02	170351.8	233745.3	1073.748
Ftk61	tswF5	6.04E+02	170320	233610	1075.735

ATTACHMENT III

Directory of files submitted to TDMS (DTN: SN9912T0511599.002)

```
12/15/99  01:55p               340,219 AMR_U0120_data.ZIP
12/13/99  03:29p                   558 README.TXT
```

ZIP file AMR_U0120_data.ZIP contains the following files:

AMR_U0120_Weep_data.ZIP	11/29/1999 12:24 PM	219,005	Weep-spacing files (Sect. 6.3.3)
README.TXT	12/13/1999 3:29 PM	558	
Readme.weep	11/29/1999 12:24 PM	1,133	
Seep-sr.xls	12/15/1999 1:54 PM	419,328	Seepage-abstraction spreadsheet
Seepage_Abstraction.txt	12/13/1999 3:22 PM	2,736	Seepage-abstraction summary

ZIP file AMR_U0120_Weep_data.ZIP contains the following files, all related to the calculation of weep spacing (Section 6.3.3):

```
glal1_perc.qpc       11/23/1999 11:48 PM  57,430  pa_glal1_weep\
glal1_weep.out       11/22/1999 3:30 PM   30,223  pa_glal1_weep\
glal1_weep.QDA       11/23/1999 11:49 PM  33,368  pa_glal1_weep\
glal1_weep1_log.qpc  11/23/1999 11:43 PM  58,320  pa_glal1_weep\
glal1_weep2_log.qpc  11/23/1999 11:47 PM  57,790  pa_glal1_weep\
glam1_perc.QPC       11/23/1999 11:47 PM  54,392  pa_glam1_weep\
glam1_weep.out       11/22/1999 3:30 PM   30,223  pa_glam1_weep\
glam1_weep.QDA       11/23/1999 11:58 PM  33,368  pa_glam1_weep\
glam1_weep1_log.qpc  11/23/1999 11:59 PM  57,860  pa_glam1_weep\
glam1_weep2_log.qpc  11/24/1999 12:00 AM  57,776  pa_glam1_weep\
glau1_perc.qpc       11/24/1999 12:06 AM  58,004  pa_glau1_weep\
glau1_weep.out       11/22/1999 3:30 PM   30,223  pa_glau1_weep\
glau1_weep.QDA       11/24/1999 12:01 AM  33,368  pa_glau1_weep\
glau1_weep1_log.qpc  11/24/1999 12:02 AM  58,162  pa_glau1_weep\
glau1_weep2_log.qpc  11/24/1999 12:17 AM  58,170  pa_glau1_weep\
Readme               11/23/1999 6:01 PM      556  pa_glal1_weep\
Readme               11/23/1999 6:01 PM      556  pa_glam1_weep\
Readme               11/23/1999 6:01 PM      556  pa_glau1_weep\
README.txt           11/29/1999 10:53 AM   1,133
SR-repo-nodes        11/29/1999 10:55 AM   1,930  repo-nodes\
t2weep_v1.f          11/23/1999 11:32 AM  13,073  SourceFiles\
weep.inp             11/22/1999 3:30 PM    1,607  pa_glal1_weep\
weep.inp             11/22/1999 3:30 PM    1,607  pa_glam1_weep\
weep.inp             11/22/1999 3:30 PM    1,607  pa_glau1_weep\
weep.out             11/22/1999 3:30 PM      792  pa_glal1_weep\
weep.out             11/22/1999 3:30 PM      792  pa_glam1_weep\
weep.out             11/22/1999 3:30 PM      792  pa_glau1_weep\
```